

Histone H3 threonine 11 phosphorylation is catalyzed directly by the meiosis-specific kinase Mek1 and provides a molecular readout of Mek1 activity *in vivo*

Ryan Kniewel^{1,2,†}, Hajime Murakami¹, Yan Liu^{3,††}, Nancy M. Hollingsworth³, and Scott Keeney^{1,2,4 *}

¹Molecular Biology Program, Memorial Sloan Kettering Cancer Center, New York, New York, USA

²Weill Cornell Graduate School of Medical Sciences, New York, New York, USA

³Department of Biochemistry and Cell Biology, Stony Brook University, Stony Brook, New York, USA

⁴Howard Hughes Medical Institute, Memorial Sloan Kettering Cancer Center, New York, New York, USA

† Present address: Department of Environmental Biology, Centro de Investigaciones Biológicas, Consejo Superior de Investigaciones Científicas (CSIC), Madrid, Madrid, Spain

†† Present address: OCIO, Northwell Health System, New Hyde Park, New York, USA

* Correspondence to s-keeney@ski.mskcc.org

ABSTRACT

Saccharomyces cerevisiae Mek1 is a CHK2/Rad53-family kinase that regulates meiotic recombination and progression upon its activation in response to DNA double-strand breaks (DSBs). The full catalog of direct Mek1 phosphorylation targets remains unknown. Here, we show that phosphorylation of histone H3 on threonine 11 (H3 T11ph) is induced by meiotic DSBs in *S. cerevisiae* and *Schizosaccharomyces pombe*. Molecular genetic experiments in *S. cerevisiae* confirmed that Mek1 is required for H3 T11ph and revealed that phosphorylation is rapidly reversed when Mek1 kinase is no longer active. Reconstituting histone phosphorylation *in vitro* with recombinant protein demonstrated that Mek1 directly catalyzes H3 T11ph. Mutating H3 T11 to nonphosphorylatable residues conferred no detectable defects in otherwise unperturbed meiosis, although the mutations modestly reduced spore viability in certain strains where Rad51 is used for strand exchange in place of Dmc1. H3 T11ph is therefore mostly dispensable for Mek1 function. Despite its minimal role, however, H3 T11ph is an excellent candidate for a marker of ongoing Mek1 kinase activity *in vivo*. We therefore used anti-H3 T11ph chromatin immunoprecipitation followed by deep sequencing (ChIP-seq) to examine the genome-wide spatial disposition of Mek1 kinase activity. H3 T11ph was highly enriched at presumed sites of attachment of chromatin to chromosome axes, and also gave a weaker signal that was highly localized at hotspots for DSB formation. These findings indicate that Mek1 provides functional communication between axes and the sites where recombination is occurring, thus providing insight into the higher order organization of recombining meiotic chromosomes.

INTRODUCTION

Meiotic recombination initiates with DNA double-strand breaks (DSBs) made by the topoisomerase-like transesterase Spo11 (Lam and Keeney 2014). DSBs occur throughout the genome, often, but not always, in hotspots that in *Saccharomyces cerevisiae* mostly overlap with nucleosome-depleted transcription promoters (Pan *et al.* 2011). Repair of meiotic DSBs by recombination helps form physical connections between homologous chromosomes that allow the chromosomes to segregate accurately at the first meiotic division (Hunter 2015). Because recombination defects can lead to mutations and/or aneuploidy, meiotic DSB repair is highly regulated (Subramanian and Hochwagen 2014; Hunter 2015).

A critical component of this regulation in yeast is Mre4/Mek1, a meiosis-specific homolog of the Rad53 checkpoint effector kinase (Rockmill and Roeder 1991; Leem and Ogawa 1992). In response to Spo11-generated DSBs, the kinases Tel1 and/or Mec1 (homologs of mammalian ATM and ATR, respectively) become activated and phosphorylate the chromosome axis-associated protein Hop1 among other substrates (Carballo *et al.* 2008; Cheng *et al.* 2013; Penedos *et al.* 2015). The FHA (Forkhead-associated) domain of Mek1 then binds phosphorylated Hop1, resulting in Mek1 recruitment to chromosome axes where Mek1 undergoes activation (involving trans-autophosphorylation on T327 in its activation loop) and stabilizes Hop1 phosphorylation via positive feedback (Niu *et al.* 2005; Niu *et al.* 2007; Carballo *et al.* 2008; Chuang *et al.* 2012; Penedos *et al.* 2015). Activated Mek1 promotes inter-homolog bias in recombination, that is, the preferential use of a homologous chromosome rather than sister chromatid as the template for DSB repair (Niu *et al.* 2005; Carballo *et al.* 2008; Goldfarb and Lichten 2010; Kim *et al.* 2010; Hong *et al.* 2013; Lao *et al.* 2013; Subramanian *et al.* 2016). Mek1 does so in part by phosphorylating the Rad54 protein on threonine 132 (T132) (Niu *et al.* 2007; Niu *et al.* 2009). Rad54 is a member of the Swi2/Snf2 DNA-dependent-ATPase chromatin remodeling family and is a binding partner of the strand exchange protein Rad51 (Heyer *et al.* 2006). Mek1-dependent phosphorylation of Rad54 attenuates the interaction with Rad51, allowing the meiosis-specific strand exchange protein Dmc1 to predominate (Niu *et al.* 2009). Mek1 also directly phosphorylates the T40 residue of Hed1; this stabilizes the Hed1 protein and thereby promotes its function as a negative regulator of Rad51 strand exchange activity (Callender *et al.* 2016). Mek1 also promotes the repair of interhomolog strand invasion intermediates through a pathway required for chromosome synapsis and the generation of crossovers whose distribution shows interference (Chen *et al.* 2015).

The full array of direct Mek1 phosphorylation substrates remains unknown, as only three direct targets have been definitively proven thus far: Mek1 itself, Rad54, and Hed1 (Niu *et al.* 2007; Niu *et al.* 2009; Callender *et al.* 2016). Additional Mek1-dependent phospho-proteins have been identified by mass spectrometry and other approaches, including T11 of histone H3 (Govin *et al.* 2010; Suhandynata *et al.* 2016). However, a number of Mek1-dependent phosphorylation events are known or suspected to be indirect (Suhandynata *et al.* 2016). For example, Mek1 is required for phosphorylation of the synaptonemal complex protein Zip1, but the kinase directly responsible is Cdc7-Dbf4, not Mek1 (Chen *et al.* 2015). Moreover, H3 T11 phosphorylation has been reported as being catalyzed in vegetative cells by other kinases [the pyruvate kinases Pyk1 and, to a lesser extent, Pyk2 (Li *et al.* 2015)], which might themselves be regulated by Mek1 in meiosis. Therefore, whether H3 T11 is a direct substrate for Mek1 remains to be established.

Mek1 activity plays out in the context of elaborate higher order chromosome structures. Early in meiotic prophase, sister chromatids form co-oriented arrays of DNA loops that are anchored along a linear proteinaceous axis (Zickler and Kleckner 1999; Kleckner 2006). Prominent components of these axes include sister chromatid cohesion proteins (including the meiosis-specific Rec8 subunit), Mek1, Hop1, and another meiosis-specific chromosome structural protein, Red1. Sister chromatid cohesion is established early in meiosis dependent on a

meiosis-specific cohesin subunit, Rec8 (Smith and Roeder 1997; Bailis and Roeder 1998; Klein *et al.* 1999; Panizza *et al.* 2011).

In cytological experiments, immunostaining foci of recombination proteins are axis-associated, indicating that recombination occurs in proximity to axes (reviewed in Zickler and Kleckner 2015). However, there is a strong anticorrelation between the DNA sequences preferentially bound by axis proteins (Rec8, Hop1, Red1) and the DNA sequences that often experience Spo11-induced DSBs, which suggests that recombination usually involves the DNA in chromatin loops rather than the DNA embedded in axes (Gerton *et al.* 2000; Blat *et al.* 2002; Pan *et al.* 2011; Panizza *et al.* 2011). To reconcile this paradox, the “tethered-loop/axis complex” (TLAC) model proposes that DNA segments residing on chromatin loops incur DSBs but are recruited, or tethered, to axes by interactions between recombination proteins and axis proteins (Kleckner 2006; Panizza *et al.* 2011). The TLAC model provides a framework for understanding spatial organization of recombining chromosomes, but there is as yet little direct molecular data demonstrating the proposed functional interactions between axes and DSB sites.

How Mek1 fits into this proposed organization also remains unknown. Immunocytology places Mek1 protein on axes (Bailis and Roeder 1998; Subramanian *et al.* 2016), as does dependence of Mek1 activity on axis proteins (Niu *et al.* 2007; Carballo *et al.* 2008), but Mek1 exerts its known recombination-controlling activity (directly or indirectly) at sites of DSBs. The TLAC model can account for Mek1 acting at both places, but where Mek1 kinase activity actually occurs remains unexplored because of a lack of a molecular marker for the active kinase.

In this study we demonstrate that Mek1 directly phosphorylates histone H3 T11 in response to meiotic DSBs in *S. cerevisiae*. H3 T11ph is dispensable for Mek1 function during unperturbed meiosis, so the purpose of this phosphorylation event remains unclear. Nevertheless, we demonstrate the utility of H3 T11ph as a molecular marker for active Mek1. Studies of the genome-wide localization of H3 T11ph indicate functional communication between chromosome axes and the sites where DSBs normally are formed, consistent with predictions of the TLAC model.

MATERIALS AND METHODS

Strains and histone mutagenesis strategy

S. cerevisiae and *S. pombe* strains are listed in **Supplemental Table S1**. *S. pombe* strains were generously provided by G. Smith, Fred Hutchinson Cancer Research Center. Histone gene deletion strains and plasmids expressing H3 T11 mutants from Govin et al. (2010) were generously provided by S. Berger, University of Pennsylvania. *S. cerevisiae* strains were of the SK1 strain background. Because of concerns about effects of plasmid (in)stability on the ability to score phenotypes of histone mutants and to reliably measure meiotic parameters because of cell-to-cell heterogeneity within a culture (see Results), we opted to avoid plasmid shuffle systems that have been used by others (Ahn *et al.* 2005a; Govin *et al.* 2010). Instead, strategies involving stable integration or gene replacement were employed, as follows.

Histone gene replacements: *S. cerevisiae* histone genes are arranged in divergently oriented pairs expressing either H3 and H4 or H2A and H2B; there are two of each pair, i.e., two copies encoding each histone. The S10A and T11V mutations were introduced into plasmid-borne copies of *HHT1* and *HHT2* by QuikChange site-directed mutagenesis (Agilent Technologies). These mutant alleles were then introduced sequentially into SK1 strain SKY165 by one-step gene replacements using DNA fragments containing ≥ 270 bp arms of homology. Targeting constructs included selectable drug resistance markers: *kanMX4* ~366 bp downstream of the *HHT1* ORF and *hphMX4* ~250 bp downstream of *HHT2*.

Stable integration of histone gene cassettes: A histone cassette integration strategy was employed using pRS305-based plasmids (Sikorski and Hieter 1989) integrated into the *leu2::hisG* locus in SK1 strains. Integrations were performed so as to try to maintain balanced gene dosage for the four core histones. The parental strain for the H2A/H2B/H3/H4 histone cassette integrations was created in a multistep process by first transforming a pRS316-based *URA3* histone cassette covering plasmid containing a single copy of each histone gene (pRK12; *HTA1-HTB1*, *HHT2-HHF2*) into diploid SKY165. Next, the histone gene pairs, *HHT2-HHF2* and *HTA1-HTB1* (which are required for proper meiosis (Norris and Osley 1987)), were deleted sequentially and replaced with the *hphMX* and *natMX* markers, respectively. The deletions were confirmed by Southern blot and the strain was sporulated to yield a Ura^+ , Nat^R , Hyg^R , *MAT α* haploid. A second *MAT α* haploid strain was created by sequentially deleting the other (non-essential) histone gene pairs, *HTA2-HTB2* and *HHT1-HHF1*, which were replaced by the *kanMX* and *natMX* markers, respectively, and confirmed by Southern blot. These two haploids were mated to form a compound heterozygote, then tetrads were dissected and resulting haploids carrying all four histone gene-pair deletions were mated to form a histone integration host strain (SKY2283) with the genotype: *hht1-hhf1 Δ ::kanMX/*, *hht2-hhf2 Δ ::natMX/*, *hta1-htb1 Δ ::hphMX/*, *hta2-htb2 Δ ::natMX/*, *pRK12[CEN/ARS, URA3, HTA1-HTB1, HHF2-HHT2]*.

A parental strain for the H3/H4 histone cassette integrations was created by dissecting tetrads from the *hht2-hhf2 Δ ::natMX/*, *pRK12* strain described above prior to deletion of *HTA1-HTB1*. This dissection yielded a Ura^+ , Nat^R , *MAT α* haploid that was crossed with the second haploid strain described above (*hta2-htb2 Δ ::natMX*, *hht1-hhf1 Δ ::kanMX*). Tetrad dissection yielded *MAT α* and *MAT α* haploid progeny (SKY3166 and SKY3167, respectively) with the following genotype: *hht1-hhf1 Δ ::kanMX*, *hhf2-hht2 Δ ::natMX*, *hta2-htb2 Δ ::natMX*, *pRK12*.

All histone mutant integration constructs were created by QuikChange site-directed mutagenesis. The first was a H3/H4 replacement using a pRS305-based plasmid (pRK77) containing *LEU2*, *HHT2-HHF2* that was linearized by AflII digestion to target integration to *leu2::hisG* and transformed into haploids SKY3166 and SKY3167. The second was an H2A/H2B/H3/H4 replacement using a pRS305-based plasmid (pRK24) containing *LEU2*, *HTA1-HTB1* and *HHF2-HHT2* that was linearized by AflII digestion and transformed into diploid SKY2283. In both cases, the core-histone covering plasmid pRK12 was counterselected by

growth on 5-fluoroorotic acid (FOA). Colony PCR of Leu^+ , Ura^- transformants was used to verify the proper integration into the *leu2::hisG* locus using primer sets flanking both junctions as well as verification of the mutations in *hta1* and *hht2* by engineered restriction enzyme site polymorphisms and/or sequencing. In the case of the SKY3166/3167 transformants, haploid integrants were subsequently mated to create diploids. SKY2283 hemizygous integrants were sporulated to produce haploid progeny that were then mated to create homozygous diploids.

***S. cerevisiae* and *S. pombe* cultures**

S. cerevisiae was cultured at 30°C with asynchronous vegetative (cycling) cultures in YPD (1% yeast extract, 2% peptone, 2% dextrose). Camptothecin treatment (20 μ M) was performed for 2 hr at 30°C in 250 ml flasks shaking at 250 rpm in 10 ml cultures of SKY165 at an initial cell density of $\sim 9 \times 10^7$ cells/ml. An untreated culture was incubated in parallel, while a separate 10 ml aliquot in a vented T-75 flask was exposed to X-rays for 60 min at room temperature using an X-RAD 225C X-ray irradiator (Precision X-ray, Inc.) corresponding to a dose of 400 Gy. Alternatively, 10 ml of culture at $\sim 7 \times 10^7$ cells/ml was exposed to X-rays for 60 min on ice, with untreated cells also held on ice. With both exposure conditions, cells were subsequently allowed to recover at 30°C, shaking at 225 rpm for 60 min (room temperature exposure) or 30 min (exposure on ice) before fixing in 20% trichloroacetic acid (TCA), pelleting and storage at -80°C until extract preparation.

For inhibition of Mek1-as *in vivo*, an SKY3095 culture was divided equally four hours after transfer to sporulation medium and 10 μ l 100% DMSO was added to half while the other received 1 μ M final concentration of 1-NA-PP1 (1-(1,1-Dimethylethyl)-3-(1-naphthalenyl)-1H-pyrazolo[3,4-d]pyrimidin-4-amine) dissolved in DMSO (Wan *et al.* 2004). The return-to-growth recombination assays using *arg4* heteroalleles were carried out in triplicate as described (Martini *et al.* 2006). Pulsed-field gel electrophoresis (PFGE) and Southern blotting on DNA from meiotic cultures prepared using the SPS method was performed as described (Murakami *et al.* 2009). Plasmid shuffling and meiotic cultures using plasmids and the SK1 histone gene deletion strain obtained from S. Berger were carried out as described (Govin *et al.* 2010).

S. pombe haploid *pat1-114* sporulation was carried out as described (Hyppa and Smith 2009). For *S. cerevisiae* meiotic cultures, strains were thawed on YPG plates (1% yeast extract, 2% peptone, 3% glycerol, 2% agar) and incubated for ~ 2 days, then streaked for single colonies on YPD plates and grown ~ 2 days. Single diploid colonies were inoculated in 5 ml YPD and grown overnight. Cultures were diluted in YP+1% potassium acetate presporulation medium to $\sim 1.2 \times 10^6$ cells/ml, grown for 13.5 hours at 225 rpm for ChIP and 250 rpm for all other experiments. Cells were pelleted, washed in sterile water and resuspended in the same preculture volume of 2% potassium acetate to a density of $\sim 2-3 \times 10^7$ cells/ml. This corresponds to 0 hr of the meiotic time course. Sporulation was at 225 rpm for ChIP and 250 rpm for all other experiments. Meiotic progression was assessed in culture aliquots fixed with 50% ethanol and stained with 5 μ g/ml 4',6-diamidino-2-phenylindole (DAPI).

Whole-cell extracts and western blotting

Culture aliquots of OD₆₀₀ = 10 for *S. pombe* or $\sim 3.2 \times 10^8$ cells for *S. cerevisiae* were washed in 20% TCA, pelleted and stored at -80°C until ready for use. Aliquots were thawed, resuspended in 20% TCA and disrupted by bead beading at 4°C using 0.5 mm zirconia/silica or glass beads and monitored microscopically until near complete disruption was observed. Samples were collected by centrifugation, then washed with 5% TCA and the pellet was resuspended in 1 \times NuPAGE LDS Sample Loading Buffer (Life Technologies Corp.) with 100 mM dithiothreitol (DTT). Samples were separated on 12% bis-Tris NuPAGE gels in 1 \times MOPS or MES running buffer (Life Technologies Corp.) or 15% Laemmli gels (Laemmli 1970).

Proteins were blotted to polyvinylidene difluoride (PVDF) membranes by semi-dry electrophoretic transfer using the iBlot system (Life Technologies Corp.) or in Tris-glycine (25 mM Tris base, 192 mM glycine, 10% methanol, 0.04% sodium dodecyl sulfate) at 100 mA constant for 70 min (TransBlot SD Transfer Cell, Bio-Rad Laboratories, Inc.). Membranes were air dried, then incubated with one of the following rabbit primary antibodies diluted in 5% non-fat milk (NFM) in Tris-buffered saline-Tween buffer (TBST; 25 mM Tris-HCl pH 7.4, 137 mM NaCl, 2.7 mM KCl, 0.1% Tween 20): anti-H3 polyclonal (Abcam 1791) diluted 1:10,000; anti-H3 T11ph monoclonal (EMD Millipore 05-789) diluted 1:1000; anti-H3 T11ph polyclonal (Active Motif 39151) diluted 1:1000; anti-H3 S10ph monoclonal (EMD Millipore 05-817) diluted 1:1000; anti-H3 S10ph polyclonal (EMD Millipore 06-560) diluted 1:1000; or anti-H2A S129ph polyclonal (Abcam 15083) diluted 1:500. The polyclonal secondary antibody used was horseradish peroxidase-conjugated goat anti-rabbit (Pierce/ThermoFisher Scientific 31462 or 31460) diluted 1:10,000 in TBST with visualization by the ECL-Plus kit (GE Healthcare Ltd.) exposed to chemiluminescent film or charged-coupled device (CCD) camera (ImageStation, Eastman Kodak Company).

Validation of anti-phospho-H3 antibodies

Two commercial anti-H3 T11ph antibodies yielded Spo11-dependent bands at the expected size for H3 on western blots, but the monoclonal gave more robust signal with less background (**Figure 1B**). To more definitively characterize the specificity of these antibodies, we incubated them with synthetic peptide arrays containing different H3 modification states (Active Motif MODified histone peptide array) (**Supplemental Table S2**). The monoclonal anti-H3 T11ph antibody reacted strongly with all peptides containing T11ph regardless of other modifications present, unless S10 was also phosphorylated, in which case reactivity was strongly or completely lost (**Supplemental Figure S1Ai**). This monoclonal antibody was highly specific, as little to no cross-reactivity was observed for unmodified H3 peptides, H3 peptides carrying other modifications, or peptides from other histones, including peptides phosphorylated at other sites (H3 S10ph, H3 S28ph, H4 S1ph, H2A S1ph, H2B S14ph) (**Supplemental Figure S1Ai**). In a more limited analysis, the polyclonal anti-H3 T11ph antibody bound specifically to a peptide with trimethylated H3 K9 (K9me3) as well as T11ph, but not to unmodified or S10ph peptides from H3 or full-length unmodified histones (**Supplemental Figure S1B**). However, this polyclonal antibody showed substantial non-histone cross-reactivity against yeast whole-cell extracts that was not observed for the monoclonal anti-H3 T11ph antibody (**Figure 1B**).

Both the monoclonal and the polyclonal anti-H3 S10ph antibodies we used reacted with phospho-S10 H3 peptide on dot blots, but with some background signal for full-length histone H3 (**Supplemental Figure S1B**). Similarly, the polyclonal anti-H3 S10ph antibody detected S10ph on the peptide array, including in the context of other nearby modifications, unless T11 was also phosphorylated (**Supplemental Figure S1Aii**). Again, however, modest cross-reactivity was seen with other histone H3 and H4 peptides, thus the anti-S10ph antibodies are less specific than the monoclonal anti-T11ph antibody.

In vitro kinase assays

GST-Mek1 and GST-mek1-as were affinity purified on glutathione sepharose as described (Niu *et al.* 2009; Lo and Hollingsworth 2011).

Radiolabeling method: Reactions included 2 µg of recombinant *S. cerevisiae* histone H3 or 5 µg H3 1-20 peptides, 250 ng GST-Mek1, 0.4 mM ATP and 10 µCi [γ -³²P]-ATP (6000 Ci/mmol; PerkinElmer, Inc.) in 25 µl total volume in a buffer containing 50 mM HEPES-NaOH pH 7.5, 150 mM NaCl, 10 mM MgCl₂, 0.5 mM DTT and 1× each of Roche phosphatase and protease inhibitor cocktails. Reactions were incubated at 30°C for 30 min then resolved on 12%

bis-Tris NuPAGE gels in 1× MES running buffer and transferred to PVDF via the iBlot system or Coomassie stained and dried for autoradiography on a Fujifilm FLA 7000. Primary antibody was rabbit anti-H3 T11ph polyclonal (Active Motif 39151) diluted 1:500, with secondary antibody and detection carried out as described above.

Semi-synthetic epitope method: GST-Mek1-as target labeling and detection followed previously described methods (Niu *et al.* 2009; Lo and Hollingsworth 2011). Reactions included 2 µg of recombinant *S. cerevisiae* histone H3, 2 µg GST-Mek1 or 0.76 µg GST-Mek1-as, 0.4 mM ATPγS or 6-Fu-ATPγS (N⁶-furfuryladenine-5'-O-3-thiotriphosphate, Axxora, LLC), and 0.2 mM ATP in 25 µl total volume in a buffer containing 50 mM Tris-HCl pH 7.5, 150 mM NaCl, 10 mM MgCl₂ and 0.5 mM DTT. Reactions were incubated at 30°C for 30 min, then *p*-nitrobenzyl mesylate (PNBM in DMSO, Abcam/Epitomics 3700-1) was added to 2.5 mM and incubated at room temperature for 90 min. Samples were electrophoresed on 4–12% bis-Tris NuPAGE gels in 1× MES running buffer, followed by semi-dry transfer to PVDF at 25 V constant for 60 min. Membranes were blocked in 5% NFM-TBST, primary antibodies were rabbit anti-thiophosphate ester monoclonal (Abcam/Epitomics 2686-1) diluted 1:5000 or rabbit anti-H3 T11ph monoclonal (EMD Millipore 05-789) diluted 1:1000, with secondary antibody and detection carried out as described above.

ChIP-sequencing

The ChIP-seq protocol was based on a previously described method (Zhang *et al.* 2011). One-liter meiotic cultures of strain SKY165 (~1.9–3.2 × 10¹⁰ cells) were harvested at the 5 hr time point and fixed with 1% formaldehyde for 15 min at room temperature, with mixing at 50 rpm. Crosslinking was quenched by adding glycine to 131 mM for 5 min, cells were washed with water, resuspended in ice-cold ST buffer (10 mM Tris-HCl pH 7.4, 100 mM NaCl and 1× each of Roche phosphatase and protease inhibitor cocktails), and pelleted and frozen at -80°C. Frozen cell pellets were thawed, resuspended in FA lysis buffer (50 mM HEPES-NaOH pH 7.5, 150 mM NaCl, 2 mM EDTA, 1% Triton X-100, 0.1% sodium deoxycholate, 10 µg/ml each of leupeptin, pepstatin A and chymostatin, 1 mM PMSF, 1× each of Roche phosphatase and protease inhibitor cocktails) and dispensed into 24 to 40 aliquots of ~6.4 × 10⁸ cells each in 2 ml screw-cap tubes. Zirconia/silica beads (0.5 mm, Biospec Products, Inc. 11079105z) were added to 50% of the total volume followed by vortexing at maximum speed for 3 hr at 4°C. If needed, additional 1 min rounds of disruption using a bead beater (Mini-Beadbeater-16, Biospec Products, Inc.) were carried out at 4°C until near complete cell disruption was observed microscopically. Extracts were collected by centrifugation at 15,000 rpm for 5 min at 4°C. Pellets were washed with 0.6 ml NPS buffer (0.5 mM spermidine, 0.075% IGEPAL CA-630, 50 mM NaCl, 10 mM Tris-HCl pH 7.4, 10 mM MgCl₂, 2 mM CaCl₂, 1 mM 2-mercaptoethanol, 10 µg/ml each of leupeptin, pepstatin A and chymostatin, 1 mM PMSF, 1× each of Roche phosphatase and protease inhibitor cocktails), resuspended in 0.6 mL NP-S buffer and incubated at 37°C for 10 min, shaking 1400 rpm in a Thermomixer (Eppendorf AG). One unit of micrococcal nuclease (Worthington Biochemical Corp.) was added and incubation was continued at 37°C for 14 min, 1400 rpm. Digestion was stopped by adding EDTA to 10 µM and holding on ice for 10 min. Then, SDS was added to 0.05% followed by sonication (Biorupter Standard, Diagenode) on highest setting at 4°C for two rounds of 30 sec with a 30 sec intervening rest. Material was then centrifuged at 16,000 rpm for 10 min at 4°C, separating the sample into supernatant for IP input and pellet fractions. Diagnostic samples of both fractions were reserved (~2.6 × 10⁸ cell equivalents each).

Supernatants were pooled and divided into four or five equal volumes, then 50 µg of each antibody was added and the extracts incubated at 4°C overnight on a rotisserie mixer (Antibodies: mock, normal rabbit IgG (SantaCruz Biotechnology sc-2027); rabbit anti-H3 pAb

(Abcam 1791); rabbit anti-H3 T11ph mAb (EMD Millipore 05-789). Immunoprecipitation was carried out by adding 500 μ l protein G Dynabeads (Life Technologies Corp.) and incubating at 4° C for 90 minutes on a rotisserie mixer. Beads were then transferred to low protein binding 1.5 ml tubes and washed 9 times by adding 1 ml of the following buffers in order and incubating at room temperature for 5 min on a rotisserie mixer: NP-S buffer, FA lysis buffer, 2 \times FA high salt buffer (FA lysis buffer containing 1 M NaCl), 2 \times FA wash 2 buffer (FA lysis buffer containing 0.5 M NaCl), 2 \times FA wash 3 buffer (10 mM Tris-HCl pH 8, 250 mM LiCl, 2 mM EDTA, 1% IGEPAL, 1% sodium deoxycholate) and TE (10 mM Tris-HCl pH 8, 1 mM EDTA). Bound nucleosomes were eluted by adding 450 μ l of 25 mM Tris-HCl pH 8, 2 mM EDTA, 0.5% SDS and 200 mM NaCl and incubated at 65°C for 15 min with 30 sec intervals of 1400 rpm shaking in a Thermomixer. Eluates were transferred to low protein binding 1.5 ml tubes with 40 μ g proteinase K (PCR grade, Roche/SigmaAldrich Company) and incubated at 65°C for 15 hr to reverse crosslinks. Nucleosomal DNA was extracted using an equal volume (500 μ l) of phenol:chloroform:isoamyl alcohol (25:24:1), precipitated by the addition of 20 μ g glycogen (Roche/SigmaAldrich Company), 0.1 volumes of 3 M sodium acetate and 2 volumes of -20°C 100% ethanol followed by washing with ice-cold 70% ethanol. ChIP yields were estimated by quantifying the DNA concentrations using a Nanodrop spectrophotometer (ThermoFisher Scientific) and by resolving an aliquot on 2% agarose. Mononucleosome-sized DNA (~200 bp) was selected using the Pippin prep system (Sage Science, Inc.) and prepared for 75 nt paired-end sequencing on the HiSeq 2000 platform (Illumina, Inc.) following standard Illumina protocols. Sequencing was performed at the Integrated Genomics Operation of Memorial Sloan-Kettering Cancer Center.

Paired-end 75 nt reads were mapped to the *S. cerevisiae* reference genome, version sacCer2 2008 using Bowtie from within the Galaxy genome analysis package (Giardine *et al.* 2005; Langmead *et al.* 2009; Blankenberg *et al.* 2010; Goecks *et al.* 2010) with the maximum insert size limited to 200 nt giving 7.8 million mapped reads of 160 bp mean length for H3 IP, 4.9 million mapped reads of 153 bp mean length for H3 T11ph IP and 0.9 million mapped reads of 167 bp mean length of the mock IP. The aligned reads were converted into coverage values at each genome position and the values corresponding to the repetitive rDNA (*RDN*) locus were expunged. The coverage values for the H3 and H3 T11ph datasets were then scaled to the concentration of immunoprecipitated DNA as determined by Nanodrop spectrophotometry. Next, the ChIP coverage values at each genome position were mock-subtracted, normalized and log transformed using the following formula: $\log_2((\text{ChIP coverage} - \text{mock ChIP})/(\text{meanChIPchr} - \text{mock ChIP}) + 0.5)$, with meanChIPchr corresponding to the mean ChIP coverage value for each chromosome. All downstream analyses were carried out using R (<http://www.r-project.org/>) (R Development Core Team 2012).

RESULTS

H3 T11 phosphorylation during meiosis is a response to DSBs.

As part of a larger effort to identify meiotically regulated histone modifications in *S. cerevisiae*, we performed western blots on meiotic whole-cell extracts with antibodies to H3 T11ph. Under these conditions, signal was undetectable in mitotically cycling, premeiotic (G1-arrested, 0 hr), or early meiotic (through 2 hr) cultures, but accumulated transiently during meiosis with a maximum at ~3 to 5 h (**Figure 1Ai, 1B**). This signal diminished as cells completed the first meiotic division (~7 hr; **Figure 1Ai, 1B, 1C**). These findings agreed with studies reported while this work was in progress (Govin *et al.* 2010).

The anti-H3 T11ph signal occurred when DSBs are usually maximal under these conditions [~3 to 5 hr (e.g., Thacker *et al.* 2014)], and coincided with an increase in H2A S129 phosphorylation (γ -H2A) (**Figure 1Ai**), which is formed by Mec1 and Tel1 kinases in response to meiotic DSBs (Mahadevaiah *et al.* 2001; Shroff *et al.* 2004). These results suggested H3 T11ph might be a DSB response, but H3 T11ph signal also coincided with an increase in H3 S10 phosphorylation (**Figure 1Ai**), which is DSB-independent (Hsu *et al.* 2000; Ahn *et al.* 2005b).

We therefore examined genetic requirements for H3 T11ph. The modification was undetectable in a strain with catalytically inactive Spo11 (*spo11-Y135F*; **Figure 1Aii, 1B**). As expected, induction of higher γ -H2A signal was not seen in *spo11-Y135F*, but H3 S10ph was (**Figure 1Aii**). H3 T11ph appeared in a *rad50S* strain, in which DSBs form but persist with unresected 5' ends, so DSB resection is dispensable (**Figure 1Aiii**). H3 S10ph was unaffected in this mutant, but elevated γ -H2A levels persisted to late time points consistent with unmitigated Tel1 activity (Usui *et al.* 2001).

H3 T11ph appeared and disappeared in *rad51Δ* with kinetics similar to wild type (**Figure 1Av**), but persisted at high levels in *dmc1Δ* (**Figure 1Avi**) (a different antibody was used for these blots, discussed below). Both *rad51Δ* and *dmc1Δ* have defects in meiotic DSB repair (note the persistent γ -H2A), but with a more complete block in *dmc1Δ* (Bishop *et al.* 1992; Shinohara *et al.* 1992). Meiotic arrest is also nearly complete in *dmc1Δ*, whereas divisions occur in *rad51Δ* after a delay (**Figure 1C**) (Bishop *et al.* 1992; Shinohara *et al.* 1992).

To determine whether this persistent H3 T11ph signal was due to persistent DSBs or to meiotic arrest, we examined an *ndt80Δ* mutant. Ndt80 is a transcription factor needed for pachytene exit (Xu *et al.* 1995; Chu and Herskowitz 1998), and DSB repair defects cause arrest via checkpoint kinase-mediated inhibition of Ndt80 (Tung *et al.* 2000; Gasior *et al.* 2001). H3 T11ph did not persist in an *ndt80Δ* mutant and instead peaked at 4 h at a slightly lower level than in wild type (**Figure 1Aiv**). This agrees with a recent report demonstrating H3 T11ph appearance and disappearance by western blotting and immunofluorescence of spread chromosomes (Subramanian *et al.* 2016). Therefore, H3 T11ph persistence correlates with continued presence of meiotic DSBs (as in *dmc1Δ*), but not with arrest. In contrast, both γ -H2A and H3 S10ph persisted at high levels in *ndt80Δ* (Hsu *et al.* 2000), suggesting these modifications require pachytene exit for removal (Subramanian *et al.* 2016).

Because the H3 N-terminal tail has many potential modification sites (**Figure 1D**) and a different antibody not used in our studies cross-reacts between H3 T11ph, H3 S10ph and other modifications (Nady *et al.* 2008), we sought to validate the antibody specificity for the anti-H3 T11ph antibodies we used. Both the monoclonal and polyclonal anti-H3 T11ph antibodies were specific but did not detect H3 T11ph if S10 was also phosphorylated (**Supplemental Figure S1** and Materials and Methods). The monoclonal gave a more robust signal with less background for non-histone proteins (**Figure 1B**), so most subsequent experiments used this antibody. Two different anti-H3 S10ph antibodies recognized their cognate modification, but not if T11 was also phosphorylated. These anti-H3 S10ph antibodies showed significant cross-reactivity to other histones and modifications (**Supplemental Figure S1** and Materials and Methods).

To test if DNA lesions could also give rise to elevated T11 phosphorylation during vegetative growth, cells were treated with X-rays or camptothecin. These DNA damaging agents failed to yield a detectable level of H3 T11ph despite inducing DNA damage responses as evidenced by increased γ -H2A (**Figure 1E**). Thus, high levels of H3 T11ph are largely if not exclusively specific to meiosis. The strength of the meiotic H3 T11ph signal as compared to the undetectable levels under these blotting conditions for cycling or premeiotic cells or the *spo11-Y135F* mutant indicates that the amount of H3 T11ph formed in meiosis is vastly greater than what another study reported was due to pyruvate kinase during vegetative growth (Li *et al.* 2015).

H3 T11ph in response to DSBs in *S. pombe* meiosis

To determine if meiotic H3 T11ph is evolutionarily conserved, we analyzed synchronous meiosis in *S. pombe* haploid *pat1-114* mutants (Bahler *et al.* 1991). H3 T11ph appeared transiently at ~4–5 hr after the initiation of meiosis and was not detected in a mutant lacking Rec12 (the Spo11 homolog) or in vegetative growth (**Figure 2**). H3 T11ph appeared after a Rec12-dependent increase in γ -H2A that starts around 3–3.5 hr, when DSBs typically appear under these conditions (Cervantes *et al.* 2000). (The initial wave of γ -H2A signal at or before 2 hr is Rec12-independent (**Figure 2B**) and possibly associated with DNA replication.) These results indicate that H3 T11ph forms in response to DSBs in *S. pombe*. H3 T11ph appeared and disappeared with apparently normal kinetics in a *rad50S* mutant in contrast to γ -H2A, which persisted at high levels (**Figure 2C**).

H3 S10ph also appeared during meiosis, but unlike in *S. cerevisiae*, this modification occurred later than H3 T11ph (**Figure 2A**). In the *rec12* mutant H3 S10ph was observed earlier than normal and was largely gone by 6 hr (**Figure 2B**). This result is consistent with accelerated meiotic progression in *rec12* mutants (Doll *et al.* 2008), and indicates that both appearance and disappearance of H3 S10ph are developmentally regulated.

H3 T11 is a direct target of Mek1 kinase.

The timing and genetic control of H3 T11ph in *S. cerevisiae* suggested that a meiosis-specific, DSB-responsive kinase was responsible. Mek1 expression coincides with H3 T11ph from 3–7 hr in meiosis (Carballo *et al.* 2008), and the T11 sequence context matches the Mek1 target consensus (RXXT; **Figure 1D**) (Mok *et al.* 2010; Suhandynata *et al.* 2016)}. We therefore treated a *dmc1Δ* strain expressing an ATP-analog sensitive *mek1* allele (*mek1-as*) with an inhibitor specific for the mutated Mek1 kinase, 1-NA-PP1 (Wan *et al.* 2004). Inhibitor addition at 4 hr caused rapid disappearance of H3 T11ph within the first hour (**Figure 3A**). This result demonstrates that Mek1 activity is necessary to maintain H3 T11 phosphorylation, and further implies that this modification is dynamic with a half-life much shorter than one hour.

This result agreed with prior findings demonstrating that H3 T11ph is reduced or absent in a *mek1Δ* mutant (Govin *et al.* 2010). However, these findings did not establish whether H3 T11 is a direct target of Mek1. To address this question, we carried out two types of *in vitro* kinase assay using GST-tagged Mek1 purified from meiotic *S. cerevisiae* cells (Wan *et al.* 2004; Niu *et al.* 2007). First, we used [γ -³²P]ATP and full-length H3 or synthetic H3 peptides as substrates (**Figure 3B**). GST-Mek1 was visible in all lanes by Coomassie staining (**Figure 3B**, bottom panel) and its activity was confirmed by its ability to autophosphorylate (**Figure 3B**, top panel) (Niu *et al.* 2009). GST-Mek1 was able to phosphorylate full-length H3 and a peptide representing H3 amino acids 1-20 (**Figure 3B**, top panel, lanes 2 and 3). Phospho-transfer was specific for T11, as shown by western blot (**Figure 3B**, middle panel, lanes 2 and 3) and inability to label an H3 1-20 peptide that was already phosphorylated on T11 (**Figure 3B**, lane 5). Interestingly, GST-Mek1 was also unable to phosphorylate a peptide carrying a phosphate on

S10 (**Figure 3B**, top panel, lane 4).

The second assay used a semisynthetic epitope system (Allen *et al.* 2007) to detect phosphorylation of H3 by Mek1. GST-Mek1 or GST-Mek1-as were incubated with recombinant H3 and the ATP γ S analog, 6-Fu-ATP γ S. Thiophosphates transferred by Mek1 to substrates were then alkylated to create an epitope that could be detected on western blots with an anti-thiophosphate ester antibody (Niu *et al.* 2009; Lo and Hollingsworth 2011). Both GST-Mek1 and GST-Mek1-as exhibited autophosphorylation and phosphorylation of H3 (**Figure 3C**, lanes 2 and 5). Moreover, 1-NA-PP1 inhibited both autophosphorylation and H3 phosphorylation by GST-Mek1-as (**Figure 3C**, lane 4), ruling out the possibility of a contaminating kinase phosphorylating H3 T11. We conclude that H3 T11 is a direct substrate of Mek1.

Limitations of a plasmid shuffle system for examining histone mutants

To determine the function of H3 T11 phosphorylation, we constructed strains carrying targeted mutations of T11 alone and in combination with other histone mutations. We initially tested an existing plasmid shuffle system (Ahn *et al.* 2005a) by porting it to the SK1 strain background. In this approach, also used independently by others (Govin *et al.* 2010), the endogenous histone genes were deleted and complemented by wild-type histone genes on a *URA3*-marked *ARS-CEN* plasmid. Histone mutants were introduced on a separate *LEU2 ARS-CEN* plasmid and loss of the *URA3* plasmid was selected for on medium containing 5-FOA.

However, this approach was sub-optimal because of the poor stability of the *ARS-CEN* plasmids in SK1. For example, when liquid cultures grown under conditions selective for the plasmid were plated on solid medium, the plating efficiency for the base histone-deletion strain carrying the *URA3* covering plasmid was only $67.2\% \pm 4.9\%$ (mean \pm SD of 5 replicates). Assuming that most cells that failed to form a colony were those that had lost the plasmid because of missegregation during mitosis, it is likely that plasmid copy number per cell is highly variable in the population. Cells with one vs. two copies of an H3/H4-encoding plasmid would likely differ in total histone protein levels and/or have different imbalances with endogenous H2A/H2B. Altered histone gene dosage can cause deleterious effects (Meeks-Wagner and Hartwell 1986; Clark-Adams *et al.* 1988), so it is possible that cell-to-cell heterogeneity in histone gene copy number might mask or exacerbate the effects of histone point mutations. Furthermore, differences in copy number might have a substantial effect on variation in viability of spores (see below). Finally, although cells in the culture that have lost the histone plasmid would be inviable and therefore presumably would not sporulate, they would contribute to population average measurements in physical assays of recombination.

To circumvent these limitations, we turned to mutagenesis methods that use gene replacement or stable chromosomal integration (Materials and Methods). Stable integration is relatively rapid and obviates concerns about plasmid stability and heterogeneous gene dosage, but may not fully recapitulate expression from endogenous histone gene loci. The gene replacement strategy provides an even cleaner manipulation of histone genotype, but is more cumbersome because it requires separately mutating two histone gene loci.

Absence of H3 T11 phosphorylation causes little or no overt phenotypes by itself.

We replaced both endogenous H3 genes (*HHT1* and *HHT2*) with *hht1-S10A*, *T11V* and *hht2-S10A*, *T11V* mutant alleles to eliminate phosphorylation of both S10 and T11. This mutant expressed normal H3 protein levels and neither H3 S10ph nor H3 T11ph could be detected, as expected (**Figure 4A**, lanes 3–4). The mutant displayed normal vegetative growth (**Figure 4B**), similar to a recent report (Li *et al.* 2015). Surprisingly, however, the mutant also displayed normal spore viability (**Table 1**). Meiotic DSBs appeared in normal numbers and locations and disappeared with normal kinetics as assessed by Southern blotting of pulsed-field gels probed for

chromosome III (**Figure 4C**), and meiotic progression was not delayed (**Figure 4D**). These results indicate that most if not all meiotic events occur efficiently in the complete absence of both S10ph and T11ph.

To more easily manipulate histone mutants, we used a chromosomal integration strategy to introduce genes for just H3 and H4 as a pair (*HHT2-HHF2*) or all four core histones (*HTA1-HTB1, HHT2-HHF2*) in strains deleted for the endogenous genes for H3-H4 or all four histones. Wild-type or mutant histone genes were integrated on chromosome III at *LEU2*. Strains expressing H3 S10A, T11V, or T11A single mutant proteins or the H3 S10A T11V double mutant were examined in meiotic timecourses for H3 S10 and T11 phosphorylation (**Figure 4A**). Importantly, H3 T11 could still be phosphorylated when S10 was mutated to alanine (**Figure 4A, lanes 9–12**); the lower signal in the anti-H3 T11ph western blot could reflect reduced T11 phosphorylation or decreased antibody affinity due to the changed epitope. Similarly, mutation of H3 T11 to alanine or valine did not prevent phosphorylation of S10, as detected with the polyclonal anti-H3 S10ph antibody, although recognition by the monoclonal anti-H3 S10ph antibody was sensitive to these mutations (**Figure 4A, lanes 13–18 and 21–22**).

As with gene replacement, all of these mutants yielded timely meiotic divisions (**Figure 4D**) and spore viabilities indistinguishable from matched wild-type controls (**Table 1**). H3 T11A also supported wild-type interhomolog recombination between *arg4* heteroalleles [23 ± 1.5 Arg⁺ recombinants per 1000 viable cells for wild type (SKY3428) vs. 24 ± 0.8 for H3 T11A (SKY3431), mean \pm SD for three independent cultures]. Other mutations of H3 T11 yielded similar results: changing T11 to serine or potential phosphomimetic residues (T11D or T11E) again yielded wild-type spore viability (**Table 1**). Mutating H3 T11 also did not reduce spore viability when combined with mutation of H2A S129 [which is also by itself largely dispensable for proper meiosis (Shroff *et al.* 2004; Harvey *et al.* 2005)] or with absence of the H3 K4 methyltransferase Set1 [which governs DSB distributions (Sollier *et al.* 2004; Borde *et al.* 2009; Acquaviva *et al.* 2013; Sommermeyer *et al.* 2013)] (**Figure 4A, lanes 21–22 and Table 2**).

Mek1 is required for arrest or delay of meiotic progression when recombination is defective (Xu *et al.* 1997; Bailis and Roeder 2000). If H3 T11ph contributes substantially to this Mek1 function, then T11 mutations should alleviate some or all of the meiotic block in *rad51Δ* or *dmc1Δ* mutants. However, in cells lacking Rad51, the *H3 S10A T11V* mutation had negligible effect on either the timing or efficiency of meiotic divisions (**Figure 4E**) and failed to rescue the spore inviability (**Table 2**). This H3 mutation also failed to alleviate the more stringent arrest in a *dmc1Δ* mutant (**Figure 4E**). Thus, H3 T11ph is dispensable for this checkpoint arrest function of Mek1.

Our findings differ from a prior report of an approximately 35% decrease in spore viability with plasmid-borne *H3 T11A* single or *S10A T11A* double mutants (Govin *et al.* 2010). We obtained the published *T11A* plasmid and histone-deleted SK1 host strain (generously provided by J. Govin and S. Berger), verified the *T11A* mutation by sequencing, and carried out the plasmid shuffle. Three independent 5-FOA-resistant clones for each genotype were sporulated and tetrads dissected for wild type and *H3 T11A* side-by-side. The experiment was repeated three times by two investigators. In our hands this *H3 T11A* mutant again yielded spore viability indistinguishable from the control with a wild-type H3 plasmid (**Figure 4F and Table 1**, $p > 0.9$ by linear regression). However, unlike the normal spore viability observed in the stable integrant and gene replacement strains (**Table 1**), viability was consistently lower with plasmid-borne histone genes regardless of H3 genotype (**Figure 4F and Table 1**). A similar defect was reported previously (Govin *et al.* 2010). Furthermore, there was substantial heterogeneity in viability from experiment to experiment and between clones within each experiment (**Figure 4F and Table 1**). Within-experiment heterogeneity likely reflects stochastic culture-to-culture variability caused by plasmid instability. Between-experiment variability may reflect differences

in sporulation conditions that in turn affect plasmid stability or the sensitivity of these strains to alterations in histone gene expression.

As a counter-example, we also examined a more extreme H3 mutant in which the entire amino-terminal tail was deleted (*H3 ΔN*). The truncated histone was expressed at levels similar to full-length H3 in vegetative cells (**Figure 4A, lanes 23-24**). This mutant displayed vegetative growth defects (**Figure 4B**), delayed and less efficient meiotic divisions (**Figure 4D**), and reduced spore viability (**Table 1**; $p = 0.45$, Fisher's exact test).

H3 T11ph contributes weakly to Mek1 function in the absence of Rad54 T132 phosphorylation.

Because *H3 T11* mutations caused no overt defects on their own, we asked whether H3 T11ph might be redundant with Mek1 phosphorylation of Rad54 on T132 (Niu *et al.* 2009). A *rad54-T132A* mutation has little effect by itself, but in a *dmc1Δ* background it allows enough Rad51 activity to partially bypass arrest and produce some viable spores (Niu *et al.* 2009).

In a *rad54-T132A dmc1Δ* background, *H3 T11V* mutation significantly reduced spore viability (**Table 2**; $p = 0.021$, Fisher's exact test), with a decrease in four-spore-viable tetrads and an increase in two- and zero-viable-spore tetrads (**Figure 4G**; $p = 8.1 \times 10^{-5}$, Fisher's exact test). This segregation pattern is diagnostic of increased MI nondisjunction. In this context, *H3 T11V* gave at best only a small increase in overall meiotic division efficiency (**Figure 4E**).

These results suggest that H3 T11 phosphorylation provides a modest contribution to Mek1 function when meiotic recombination defects are encountered. Possible roles of H3 T11ph in these contexts are addressed in the Discussion. However, since the *H3 T11* mutation by itself does not detectably phenocopy a *mek1Δ* mutant, we conclude that H3 T11ph is normally dispensable for Mek1 function.

H3 T11ph is highly enriched at axis sites and more weakly at DSB hotspots.

Immunolocalization describes where Mek1 protein can be found (Bailis and Roeder 1998), but cannot reveal where Mek1 exerts its activity. We reasoned that H3 T11ph might provide a sensitive and specific molecular marker to reveal the locations of active Mek1 kinase. To test this possibility, we assessed H3 T11ph genome-wide by ChIP-seq. Mononucleosomes were liberated from formaldehyde-fixed meiotic chromatin by digestion with micrococcal nuclease (MNase) and immunoprecipitated with the anti-H3 polyclonal or anti-H3 T11ph monoclonal antibodies, then the DNA was purified and deep sequenced and reads were mapped to the yeast genome. Coverage maps were normalized to genome average (**Figure 5A, B**). For this proof-of-principle experiment, we chose a 5 hr time point when Mek1-dependent H3 T11ph was still abundant (**Figure 1B**).

H3 ChIP-seq coverage was low in promoters and showed prominent nucleosome-width peaks in coding sequences (**Figure 5B**), as expected for promoter-associated nucleosome-depleted regions (NDRs) and positioned nucleosomes in gene bodies (Jiang and Pugh 2009). At this scale, H3 T11ph ChIP coverage also showed depletion in NDRs and nucleosomal peaks at similar positions as in the H3 map. However, there was a tendency for H3 T11ph to be less depleted relative to genome average than H3 in NDRs and, conversely, for H3 T11ph signal to be lower for nucleosomes within transcription units (**Figure 5B**). When maps were zoomed out to examine larger size scales, H3 T11ph showed broadly undulating hills and valleys that were not matched in the H3 ChIP-seq (**Figure 5A**), revealing that H3 T11ph tends to be relatively enriched or depleted in domains several kb in width (**Figure 5A**, green line).

A priori, we envisioned two non-exclusive scenarios that might describe H3 T11ph localization: Enrichment at chromosome axes because that is where Mek1 protein is enriched cytologically and Mek1 interacts with axis proteins (Bailis and Roeder 1998; Wan *et al.* 2004;

Carballo *et al.* 2008); or centered on DSB hotspots because Mek1 activation is a response to DSBs and Mek1 regulates DSB repair. We found signatures of both localization patterns, albeit to substantially different quantitative levels.

To test if H3 T11ph is enriched near axes, we compared its ChIP-seq signal with the genome-wide distribution of an axis component, Red1 (Panizza *et al.* 2011). The sites where ChIP signals for Red1 and other axis proteins are enriched are generally assumed to be the chromatin loop bases that are embedded in the chromosome axis (Blat *et al.* 2002; Panizza *et al.* 2011; Sun *et al.* 2015). These sites are often but not always in intergenic regions between convergent transcription units, presumably because transcription can push cohesin along chromosomes (Lengronne *et al.* 2004; Bausch *et al.* 2007; Sun *et al.* 2015).

When centered on Red1 ChIP-chip peaks, average H3 T11ph signal formed a broad peak ~4 kb wide, strikingly similar in dimensions to the average of Red1 itself and of another axis component, Hop1 (**Figure 5C**). Furthermore, H3 T11ph ChIP-seq correlated quantitatively genome-wide with Red1 and Hop1 ChIP (**Figure 5D**). In contrast, total histone H3 ChIP-seq was not enriched in spatial register with Red1 peaks (**Figure 5C**) and correlated only weakly with Red1 or Hop1 genome wide (**Figure 5D**). We conclude that Mek1 is highly active at axis-associated sites. The spatial coincidence between H3 T11ph and Hop1/Red1 also suggests that Mek1 activity may be locally constrained, i.e., that it does not spread far beyond the axis sites where the kinase itself is bound.

To test if H3 T11ph is enriched near DSB sites, we compared its ChIP-seq signal with DSB maps generated by sequencing of Spo11-oligos (Pan *et al.* 2011; Mohibullah and Keeney 2016). When centered on Spo11-oligo hotspots, histone ChIP-seq coverage showed a complex pattern of highly localized enrichment and depletion (**Figure 5E**). The average for total histone H3 was depleted in hotspot centers and enriched across flanking regions in shallow alternating peaks and valleys (gray line in **Figure 5E**). This is the expected pattern from prior studies, reflecting the strong preference for DSBs in *S. cerevisiae* to form in promoter NDRs flanked by positioned nucleosomes (Ohta *et al.* 1994; Wu and Lichten 1994; Pan *et al.* 2011) (e.g., **Figure 5B**).

The average H3 T11ph ChIP-seq signal differed from this pattern in informative ways (black line in **Figure 5E**). H3 T11ph was depleted across hotspot centers, but to a lesser degree than for total H3. Moreover, the average H3 T11ph signal was elevated relative to total H3 across the nucleosomes immediately flanking the hotspots (**Figure 5E inset**), but was depleted relative to total H3 for regions further away (**Figure 5E**). The net result was that the difference map (H3 T11ph – H3) showed prominent enrichment across hotspot centers and into the neighboring one or two nucleosomes on either side, but was depleted in ~1–2 kb zones in the surrounding chromatin (green line in **Figure 5E**).

It should be emphasized that these histone ChIP-seq maps are normalized to genome average, so they report relative rather than absolute nucleosome coverage values. Furthermore, compared with the rest of the genome, gene promoters have lower nucleosome occupancy but are not devoid of nucleosomes. For example, some promoters contain positioned, high-occupancy nucleosomes; some contain nucleosomes but only in a fraction of the population; and some contain sub-nucleosomal histone particles (Jiang and Pugh 2009; Floer *et al.* 2010; Weiner *et al.* 2010). It follows then that the observed enrichment for H3 T11ph does not mean that there is a higher density of nucleosomes within hotspots that are being acted on by Mek1. Rather, whatever nucleosomes happen to be present within and immediately adjacent to DSB hotspots tend to be preferred targets for Mek1.

In summary, H3 T11ph is highly enriched at preferred binding sites of axis proteins, but is also more focally enriched (and to a quantitatively lesser extent) at DSB hotspots. These results indicate that Mek1 activity is greatest at chromosome axes, but can also be detected at

sites where recombination is most likely to occur. The detailed patterns and possible implications are addressed further in the Discussion.

H3 T11ph correlates with DSB frequency across large sub-chromosomal domains.

We next examined larger scale variation in H3 T11ph ChIP signal across chromosomes. H3 T11ph ChIP signals were binned in non-overlapping windows of varying sizes from 0.5 to 40 kb, then compared (Pearson's r) to Spo11-oligo densities or ChIP signals for Red1, Hop1, or Rec8 in the same bins (**Figure 5F–I**). Comparison of the [H3 T11ph – H3] difference with Spo11-oligos and the other ChIP data shows which correlations are specific for the histone modification per se (green points in **Figure 5F–I**) as opposed to underlying (background) enrichment or depletion in the bulk chromatin map (total H3; gray points in **Figure 5F–I**).

For small windows (< 2 kb), both H3 and H3 T11ph were anticorrelated with Spo11-oligo density (**Figure 5F**). This pattern is driven by strong preference for DSBs to form in NDRs. However, the [H3 T11ph – H3] difference map deviated from this anticorrelation because of the tendency for H3 T11ph to occur focally within hotspots, noted above (**Figure 5E**). With large windows in contrast, the H3 T11ph signal instead had a significant positive correlation with Spo11-oligo density, with Pearson's r values high over a range of ~25–40 kb (**Figure 5F**). (Total histone H3 also correlated positively with Spo11 oligos for unknown reasons, but this correlation was weaker, leaving a significant positive correlation with the phosphorylation-specific ChIP signal.) We interpret this pattern to indicate that subchromosomal domains tens of kb wide that experience more DSBs also incur more Mek1 activity. This finding fits with expectation if H3 T11ph is a faithful molecular reporter of DSB-provoked Mek1 kinase activity.

In contrast to the wide variation in correlation behavior depending on window size when H3 T11ph was compared Spo11-oligo density, comparisons with either Red1 or Hop1 ChIP showed strong positive correlations over all scales tested (**Figure 5G, H**). For Rec8, H3 T11ph showed a modest positive correlation for short windows and a modest negative correlation with larger windows (**Figure 5I**). These patterns can be understood as the combination of two spatial correlations with different length dependencies. At short distances (<10 kb), Mek1 activity coincides with preferred binding sites for Red1, Hop1, and Rec8 (i.e., axis sites; **Figure 5C**). At longer distances (tens of kb), the domains that are relatively DSB-rich (and thus have more Mek1 activity) are also enriched for Red1 and Hop1 but depleted for Rec8 (Blat *et al.* 2002; Pan *et al.* 2011; Panizza *et al.* 2011).

DISCUSSION

This study and others (Govin *et al.* 2010; Suhandynata *et al.* 2016) establish that H3 T11 phosphorylation is highly induced during meiosis in *S. cerevisiae*. Our findings additionally demonstrate that H3 T11ph is a direct product of DSB-induced activation of Mek1. Mek1 is conserved in *S. pombe* (Perez-Hidalgo *et al.* 2003), so it seems likely that this kinase is also responsible for H3 T11ph in fission yeast.

Mek1 appears specifically in fungal taxa, but the larger Rad53 kinase family is ubiquitous in eukaryotes (Subramanian and Hochwagen 2014). Another member of this family, CHK1, was reported to be required for H3 T11ph in mouse fibroblasts (Shimada *et al.* 2008). In this case, however, DNA damage caused a decrease in H3 T11ph levels. It remains unknown if CHK1 directly phosphorylates H3 T11 or if H3 T11ph occurs in response to DSBs in mammalian meiosis. H3 T11ph has been reported during meiosis in sciarid flies (Escriba *et al.* 2011), indicating evolutionary conservation beyond yeasts.

H3 T11 can also be directly phosphorylated by pyruvate kinase M2 in *S. cerevisiae* and mammalian cells, possibly to coordinate chromatin structure and gene expression with the cell's nutritional status (Yang *et al.* 2012; Li *et al.* 2015). In cultured human cells, H3 T11ph is also formed by protein-kinase-C-related kinase 1 near promoters of androgen receptor-modulated genes (Metzger *et al.* 2008), and by death-associated protein (DAP)-like kinase during mitosis, particularly near centromeres (Preuss *et al.* 2003). Our results establish that meiotic induction of H3 T11ph in yeasts is fundamentally distinct from these other modes of H3 T11 phosphorylation in terms of provenance and genomic distribution.

Possible functions of H3 T11ph in meiosis

Under the conditions in this study, histone mutations that eliminated H3 T11 phosphorylation caused no discernible meiotic defects by themselves. This was true with multiple independent mutagenesis strategies and numerous mutant constructs encoding different amino acid substitutions. We conclude that H3 T11ph is dispensable for meiosis under standard conditions.

Why our results differed from a previous report (Govin *et al.* 2010) remains unknown. One possibility is that the highly variable spore viability in the plasmid shuffle system fortuitously gave the incorrect appearance of a meiotic defect in the earlier study. The reported decrease in spore viability [from ~80% in the control to ~50% with *H3 T11V* (Govin *et al.* 2010)] was of comparable magnitude to experimental variability we observed with plasmid-borne histone cassettes. Alternatively, studies in the two laboratories may have had undocumented differences in sporulation conditions to which *H3 T11* mutants are specifically sensitive.

Despite H3 T11ph being dispensable in unperturbed meiosis, we did observe that blocking phosphorylation of H3 T11 modestly exacerbated the phenotype of a *dmc1Δ rad54-T132A* mutant. One interpretation is that H3 T11ph helps Mek1 maintain residual interhomolog bias when Rad51 is the sole source of strand exchange activity. In this model, increased MI nondisjunction is caused by more of the residual DSB repair being between sister chromatids, and less between homologs. This interpretation is motivated by the increased intersister recombination observed in a *rad54-T132A* mutant when Mek1 activity was inhibited, and by ability of the *rad54-T132A* mutation to rescue some spore viability in a *dmc1Δ* background but not in *dmc1Δ mek1Δ* (Niu *et al.* 2009). These findings indicated that other Mek1 targets contribute to interhomolog recombination by Rad51 when Dmc1 is missing and Rad54 cannot be phosphorylated. The recent discovery that Mek1 phosphorylates Hed1 and histone H2B make these strong candidates for additional redundancy (Callender *et al.* 2016; Suhandynata *et al.* 2016) (N.M.H., unpublished data).

If H3 T11ph does promote Mek1 function, albeit in a minor way, what might its role be? One possibility is that it is an effector of Mek1 signaling. This could be via recruitment to chromatin of proteins with phosphothreonine binding motifs such as the FHA domain, which is present in numerous proteins in *S. cerevisiae* including the recombination protein Xrs2 (Mahajan *et al.* 2008; Matsuzaki *et al.* 2008). Or, H3 T11ph might impinge on nucleosome stability, higher-order chromatin organization, or ability to install, remove, or read other histone modifications. We observed potential crosstalk between histone modifications in that H3 S10ph blocked ability of Mek1 to phosphorylate T11 on the same peptide. Crosstalk of H3 T11ph with other H3 modifications has been documented in vegetatively growing yeast [H3 K4 methylation (Li *et al.* 2015)] and in human cells [H3 K9 acetylation (Yang *et al.* 2012) and demethylation (Metzger *et al.* 2008)].

A second, non-exclusive possibility is that H3 T11ph might maintain or amplify Mek1 activity via positive feedback. For example, the FHA domain of Mek1 might bind directly to H3 T11ph in a manner that stabilizes or increases the amount of active Mek1. Both general types of role — downstream effector or feedback amplifier — are compatible with observed genetic interaction of *H3 T11* mutation with *dmc1Δ rad54-T132A*.

Spatial organization of Mek1 activity and evidence for functional communication between axes and recombination sites

Although H3 T11 can be phosphorylated by other kinases, the magnitude of the DSB- and Mek1-dependent signal combined with its rapid disappearance when Mek1 is shut off made H3 T11ph an excellent candidate for a molecular marker of ongoing Mek1 activity. Our experiments establish proof of principle for this use.

The most prominent sites of H3 T11ph, and thus of Mek1 activity, were coincident with peaks of Red1 and Hop1, i.e., presumed axis attachment sites. This pattern is not surprising given that Mek1 protein is mostly axis-associated as assessed by immunocytology (Bailis and Roeder 1998). However, immunolocalization does not reveal kinase activity per se, and could not evaluate the degree to which activity might spread in *cis*. Interestingly, the H3 T11ph distribution was essentially identical to that of Red1 and Hop1 around axis sites. This highly localized pattern contrasts with the spread of γ -H2A over tens of kb around DSBs in yeast (Shroff *et al.* 2004). The apparent local constraint on Mek1 kinase activity could be because Mek1 protein is constrained, i.e., it rarely diffuses away from axis sites once activated. More likely, however, Mek1 may be rapidly inactivated if it diffuses away and/or the phosphates that Mek1 places outside the immediate vicinity of axes might be more rapidly reversed by phosphatases.

Coincidence of Mek1 activity with axis sites raises a conundrum: DSBs do not appear to form within axis-bound DNA, yet highly localized Mek1 activity at axis sites is completely DSB-dependent and the biological function of Mek1 — Hop1/Red1-dependent control of recombination outcome — is exerted at DSB sites. This action at a distance implies some form of communication in both directions between DSB sites and axis sites. The highly localized H3 T11ph implies that this communication is unlikely to occur via continuous spreading of activated Mek1 in *cis* along chromatin.

We also observed a clear H3 T11ph signal at DSB hotspots, albeit weaker quantitatively than at axis sites. Here, H3 T11ph was even more highly localized immediately at hotspots where DSBs preferentially form on average in the population. A puzzle about this signal is that DSBs are exonucleolytically resected for ~800 nucleotides on average on both sides of the break (Zakharyevich *et al.* 2010; Mimitou *et al.* 2017); ssDNA should not be revealed in our ChIP-seq data even if it were still bound by histones. What then is the source of H3 T11-phosphorylated nucleosomes at hotspots? Likely candidates are the sister of the broken chromatid, one or both intact chromatids of the homologous chromosome with which recombination is occurring, and/or

recombination intermediates (D-loops and double Holliday junctions) if these are chromatinized. It is formally possible that some of this signal is from pyruvate kinase targeting of promoters (Li *et al.* 2015), but we consider this less likely because RNA-seq data (Brar *et al.* 2012) show that expression of the pyruvate kinase genes *PYK1* and *PYK2* is strongly down-regulated during meiosis. Furthermore, our western blotting showed that Mek1-independent H3 T11ph, if present under our culture conditions, was extremely low abundance compared to Mek1-dependent signal. Because Mek1 controls homolog bias, we speculate that some or all of the H3 T11ph signal at hotspots is from Mek1 action on the sisters of broken chromatids. If so, the highly localized H3 T11ph distribution fits with models in which one end of each DSB associates with the unbroken sister chromatid via strand invasion or some other stable interaction (Oh *et al.* 2007; Kim *et al.* 2010; Brown and Bishop 2014).

One possible interpretation of the H3 T11ph patterns is that active Mek1 localizes independently both to axis sites and to hotspots. However, this model seems unlikely because Hop1 and Red1 are essential for Mek1 activity (e.g., Niu *et al.* 2007) but DSB hotspots are not sites where Hop1 and Red1 are enriched (in fact, just the opposite) (Panizza *et al.* 2011). Furthermore, independent localization would provide no clear explanation for how DSBs can activate Mek1 at axis sites.

An alternative interpretation is provided by the TLAC model (see Introduction). The direct interactions between axes and sites of recombination proposed by this model provide a straightforward explanation for the apparent communication at a distance we observed between Hop1/Red1 peaks and DSB hotspots. Furthermore, current versions of the TLAC model favor the idea that tethering occurs before DSB formation because some partners of Spo11 are enriched at axis sites rather than at hotspots but can be connected to hotspots physically via interactions with a reader (Spp1) of the H3 K4 methylation that is prominent around promoters (Panizza *et al.* 2011; Acquaviva *et al.* 2013; Sommermeyer *et al.* 2013). Such loop-axis interactions prior to DSB formation could provide a means to rapidly and specifically activate Mek1 at a nearby axis site in response to a DSB at a hotspot within a tethered loop.

In summary, the detection of H3 T11ph is useful as an indicator of meiotic DSB formation, an indicator of Mek1 activation level, and a marker of the spatial organization of chromatin that Mek1 acts upon. H3 T11ph ChIP will be a powerful tool for dissecting not only the function of Mek1 but also the higher order structural organization of recombining chromosomes.

ACKNOWLEDGMENTS

We thank G. Smith (Fred Hutchinson Cancer Research Center) for *S. pombe* strains and advice on culturing; J. Govin and S. Berger (University of Pennsylvania) for providing histone mutant plasmids and strains and for communicating information prior to publication; C. Hughes and C.D. Allis (Rockefeller University) for providing peptides, recombinant histones, plasmids and valuable guidance; Neil Hunter at the University of California-Davis for the *rad51Δ* strain; A. Viale, J. Cheng, L. Sun and J. Li (MSKCC Integrated Genomics Operation) for sequencing ; and N. Socci (MSKCC Bioinformatics Core) for bioinformatics assistance. MSKCC core facilities were supported by NIH/NCI Cancer Center Support Grant P30 CA008748. R.K. was supported in part by NIGMS predoctoral training award T32 BM008539. This work was supported by NIH grants R01 GM058673 and R35 GM118092 (to S.K.) and R01 GM050717 (to N.H.).

REFERENCES

- Acquaviva, L., L. Szekvolgyi, B. Dichtl, B. S. Dichtl, C. de La Roche Saint Andre *et al.*, 2013 The COMPASS subunit Spp1 links histone methylation to initiation of meiotic recombination. *Science* 339: 215-218.
- Ahn, S. H., W. L. Cheung, J. Y. Hsu, R. L. Diaz, M. M. Smith *et al.*, 2005a Sterile 20 kinase phosphorylates histone H2B at serine 10 during hydrogen peroxide-induced apoptosis in *S. cerevisiae*. *Cell* 120: 25-36.
- Ahn, S. H., K. A. Henderson, S. Keeney and C. D. Allis, 2005b H2B (Ser10) phosphorylation is induced during apoptosis and meiosis in *S. cerevisiae*. *Cell cycle (Georgetown, Tex)* 4: 780-783.
- Allen, J. J., M. Li, C. S. Brinkworth, J. L. Paulson, D. Wang *et al.*, 2007 A semisynthetic epitope for kinase substrates. *Nature methods* 4: 511-516.
- Bahler, J., P. Schuchert, C. Grimm and J. Kohli, 1991 Synchronized meiosis and recombination in fission yeast: observations with *pat1-114* diploid cells. *Current genetics* 19: 445-451.
- Bailis, J. M., and G. S. Roeder, 1998 Synaptonemal complex morphogenesis and sister-chromatid cohesion require Mek1-dependent phosphorylation of a meiotic chromosomal protein. *Genes Dev* 12: 3551-3563.
- Bailis, J. M., and G. S. Roeder, 2000 Pachytene exit controlled by reversal of Mek1-dependent phosphorylation. *Cell* 101: 211-221.
- Bausch, C., S. Noone, J. M. Henry, K. Gaudenz, B. Sanderson *et al.*, 2007 Transcription alters chromosomal locations of cohesin in *Saccharomyces cerevisiae*. *Mol Cell Biol* 27: 8522-8532.

- Bishop, D. K., D. Park, L. Xu and N. Kleckner, 1992 *DMC1*: a meiosis-specific yeast homolog of *E. coli recA* required for recombination, synaptonemal complex formation, and cell cycle progression. *Cell* 69: 439-456.
- Blankenberg, D., G. Von Kuster, N. Coraor, G. Ananda, R. Lazarus *et al.*, 2010 Galaxy: a web-based genome analysis tool for experimentalists. *Curr Protoc Mol Biol* Chapter 19: Unit 19 10 11-21.
- Blat, Y., R. U. Protacio, N. Hunter and N. Kleckner, 2002 Physical and functional interactions among basic chromosome organizational features govern early steps of meiotic chiasma formation. *Cell* 111: 791-802.
- Borde, V., N. Robine, W. Lin, S. Bonfils, V. Géli *et al.*, 2009 Histone H3 lysine 4 trimethylation marks meiotic recombination initiation sites. *EMBO J* 28: 99-111.
- Brar, G. A., M. Yassour, N. Friedman, A. Regev, N. T. Ingolia *et al.*, 2012 High-resolution view of the yeast meiotic program revealed by ribosome profiling. *Science* 335: 552-557.
- Brown, M. S., and D. K. Bishop, 2014 DNA strand exchange and RecA homologs in meiosis. *Cold Spring Harbor perspectives in biology* 7: a016659.
- Callender, T. L., R. Laureau, L. Wan, X. Chen, R. Sandhu *et al.*, 2016 Mek1 down regulates Rad51 activity during yeast meiosis by phosphorylation of Hed1. *PLoS genetics* 12: e1006226.
- Carballo, J. A., A. L. Johnson, S. G. Sedgwick and R. S. Cha, 2008 Phosphorylation of the axial element protein Hop1 by Mec1/Tel1 ensures meiotic interhomolog recombination. *Cell* 132: 758-770.
- Cervantes, M. D., J. A. Farah and G. R. Smith, 2000 Meiotic DNA breaks associated with recombination in *S. pombe*. *Mol Cell* 5: 883-888.
- Chen, X., R. T. Suhandynata, R. Sandhu, B. Rockmill, N. Mohibullah *et al.*, 2015 Phosphorylation of the synaptonemal complex protein Zip1 regulates the crossover/noncrossover decision during yeast meiosis. *PLoS Biol* 13: e1002329.
- Cheng, Y. H., C. N. Chuang, H. J. Shen, F. M. Lin and T. F. Wang, 2013 Three distinct modes of Mec1/ATR and Tel1/ATM activation illustrate differential checkpoint targeting during budding yeast early meiosis. *Mol Cell Biol* 33: 3365-3376.
- Chu, S., and I. Herskowitz, 1998 Gametogenesis in yeast is regulated by a transcriptional cascade dependent on Ndt80. *Mol Cell* 1: 685-696.
- Chuang, C. N., Y. H. Cheng and T. F. Wang, 2012 Mek1 stabilizes Hop1-Thr318 phosphorylation to promote interhomolog recombination and checkpoint responses during yeast meiosis. *Nucleic Acids Res* 40: 11416-11427.

- Clark-Adams, C. D., D. Norris, M. A. Osley, J. S. Fassler and F. Winston, 1988 Changes in histone gene dosage alter transcription in yeast. *Genes Dev.* 2: 150-159.
- Doll, E., M. Molnar, G. Cuanoud, G. Octobre, V. Latypov *et al.*, 2008 Cohesin and recombination proteins influence the G1-to-S transition in azygotic meiosis in *Schizosaccharomyces pombe*. *Genetics* 180: 727-740.
- Escriba, M. C., M. C. Giardini and C. Goday, 2011 Histone H3 phosphorylation and non-disjunction of the maternal X chromosome during male meiosis in sciarid flies. *J Cell Sci* 124: 1715-1725.
- Floer, M., X. Wang, V. Prabhu, G. Berrozpe, S. Narayan *et al.*, 2010 A RSC/nucleosome complex determines chromatin architecture and facilitates activator binding. *Cell* 141: 407-418.
- Gasior, S. L., H. Olivares, U. Ear, D. M. Hari, R. Weichselbaum *et al.*, 2001 Assembly of RecA-like recombinases: distinct roles for mediator proteins in mitosis and meiosis. *Proc Natl Acad Sci U S A* 98: 8411-8418.
- Gerton, J. L., J. DeRisi, R. Shroff, M. Lichten, P. O. Brown *et al.*, 2000 Inaugural article: global mapping of meiotic recombination hotspots and coldspots in the yeast *Saccharomyces cerevisiae*. *Proceedings of the National Academy of Sciences of the United States of America* 97: 11383-11390.
- Giardine, B., C. Riemer, R. C. Hardison, R. Burhans, L. Elnitski *et al.*, 2005 Galaxy: a platform for interactive large-scale genome analysis. *Genome Res* 15: 1451-1455.
- Goecks, J., A. Nekrutenko and J. Taylor, 2010 Galaxy: a comprehensive approach for supporting accessible, reproducible, and transparent computational research in the life sciences. *Genome Biol* 11: R86.
- Goldfarb, T., and M. Lichten, 2010 Frequent and efficient use of the sister chromatid for DNA double-strand break repair during budding yeast meiosis. *PLoS Biol* 8: e1000520.
- Govin, J., J. Dorsey, J. Gaucher, S. Rousseaux, S. Khochbin *et al.*, 2010 Systematic screen reveals new functional dynamics of histones H3 and H4 during gametogenesis. *Genes Dev* 24: 1772-1786.
- Harvey, A. C., S. P. Jackson and J. A. Downs, 2005 *Saccharomyces cerevisiae* histone H2A Ser122 facilitates DNA repair. *Genetics* 170: 543-553.
- Heyer, W. D., X. Li, M. Rolfmeier and X. P. Zhang, 2006 Rad54: the Swiss Army knife of homologous recombination? *Nucleic Acids Res* 34: 4115-4125.
- Hong, S., Y. Sung, M. Yu, M. Lee, N. Kleckner *et al.*, 2013 The logic and mechanism of homologous recombination partner choice. *Mol Cell* 51: 440-453.

- Hsu, J. Y., Z. W. Sun, X. Li, M. Reuben, K. Tatchell *et al.*, 2000 Mitotic phosphorylation of histone H3 is governed by Ipl1/aurora kinase and Glc7/PP1 phosphatase in budding yeast and nematodes. *Cell* 102: 279-291.
- Hunter, N., 2015 Meiotic recombination: The essence of heredity. Cold Spring Harbor perspectives in biology 7.
- Hyppa, R. W., and G. R. Smith, 2009 Using *Schizosaccharomyces pombe* meiosis to analyze DNA recombination intermediates. *Methods Mol Biol* 557: 235-252.
- Jiang, C., and B. F. Pugh, 2009 Nucleosome positioning and gene regulation: advances through genomics. *Nat Rev Genet* 10: 161-172.
- Kim, K. P., B. M. Weiner, L. Zhang, A. Jordan, J. Dekker *et al.*, 2010 Sister cohesion and structural axis components mediate homolog bias of meiotic recombination. *Cell* 143: 924-937.
- Kleckner, N., 2006 Chiasma formation: chromatin/axis interplay and the role(s) of the synaptonemal complex. *Chromosoma* 115: 175-194.
- Klein, F., P. Mahr, M. Galova, S. B. Buonomo, C. Michaelis *et al.*, 1999 A central role for cohesins in sister chromatid cohesion, formation of axial elements, and recombination during yeast meiosis. *Cell* 98: 91-103.
- Laemmli, U. K., 1970 Cleavage of structural proteins during the assembly of the head of bacteriophage T4. *Nature* 227: 680-685.
- Lam, I., and S. Keeney, 2014 Mechanism and regulation of meiotic recombination initiation. Cold Spring Harbor perspectives in biology 7: a016634.
- Langmead, B., C. Trapnell, M. Pop and S. L. Salzberg, 2009 Ultrafast and memory-efficient alignment of short DNA sequences to the human genome. *Genome Biol* 10: R25.
- Lao, J. P., V. Cloud, C. C. Huang, J. Grubb, D. Thacker *et al.*, 2013 Meiotic crossover control by concerted action of Rad51-Dmc1 in homolog template bias and robust homeostatic regulation. *PLoS genetics* 9: e1003978.
- Leem, S. H., and H. Ogawa, 1992 The *MRE4* gene encodes a novel protein kinase homologue required for meiotic recombination in *Saccharomyces cerevisiae*. *Nucleic Acids Res* 20: 449-457.
- Lengronne, A., Y. Katou, S. Mori, S. Yokobayashi, G. P. Kelly *et al.*, 2004 Cohesin relocation from sites of chromosomal loading to places of convergent transcription. *Nature* 430: 573-578.
- Li, S., S. K. Swanson, M. Gogol, L. Florens, M. P. Washburn *et al.*, 2015 Serine and SAM responsive complex SESAME regulates histone modification crosstalk by sensing cellular metabolism. *Mol Cell* 60: 408-421.

- Lo, H. C., and N. M. Hollingsworth, 2011 Using the semi-synthetic epitope system to identify direct substrates of the meiosis-specific budding yeast kinase, Mek1. *Methods Mol Biol* 745: 135-149.
- Mahadevaiah, S. K., J. M. Turner, F. Baudat, E. P. Rogakou, P. de Boer *et al.*, 2001 Recombinational DNA double-strand breaks in mice precede synapsis. *Nat Genet* 27: 271-276.
- Mahajan, A., C. Yuan, H. Lee, E. S. Chen, P. Y. Wu *et al.*, 2008 Structure and function of the phosphothreonine-specific FHA domain. *Sci Signal* 1: re12.
- Martini, E., R. L. Diaz, N. Hunter and S. Keeney, 2006 Crossover homeostasis in yeast meiosis. *Cell* 126: 285-295.
- Matsuzaki, K., A. Shinohara and M. Shinohara, 2008 Forkhead-associated domain of yeast Xrs2, a homolog of human Nbs1, promotes nonhomologous end joining through interaction with a ligase IV partner protein, Lif1. *Genetics* 179: 213-225.
- Meeks-Wagner, D., and L. H. Hartwell, 1986 Normal stoichiometry of histone dimer sets is necessary for high fidelity of mitotic chromosome transmission. *Cell* 44: 43-52.
- Metzger, E., N. Yin, M. Wissmann, N. Kunowska, K. Fischer *et al.*, 2008 Phosphorylation of histone H3 at threonine 11 establishes a novel chromatin mark for transcriptional regulation. *Nature cell biology* 10: 53-60.
- Mimitou, E. P., S. Yamada and S. Keeney, 2017 A global view of meiotic double-strand break end resection. *Science* 355: 40-45.
- Mohibullah, N., and S. Keeney, 2016 Numerical and spatial patterning of yeast meiotic DNA breaks by Tel1. *Genome Res.*
- Mok, J., P. M. Kim, H. Y. Lam, S. Piccirillo, X. Zhou *et al.*, 2010 Deciphering protein kinase specificity through large-scale analysis of yeast phosphorylation site motifs. *Sci Signal* 3: ra12.
- Murakami, H., V. Borde, A. Nicolas and S. Keeney, 2009 Gel electrophoresis assays for analyzing DNA double-strand breaks in *Saccharomyces cerevisiae* at various spatial resolutions. *Methods Mol Biol* 557: 117-142.
- Nady, N., J. Min, M. S. Kareta, F. Chedin and C. H. Arrowsmith, 2008 A SPOT on the chromatin landscape? Histone peptide arrays as a tool for epigenetic research. *Trends Biochem Sci* 33: 305-313.
- Niu, H., X. Li, E. Job, C. Park, D. Moazed *et al.*, 2007 Mek1 kinase is regulated to suppress double-strand break repair between sister chromatids during budding yeast meiosis. *Mol Cell Biol* 27: 5456-5467.

- Niu, H., L. Wan, B. Baumgartner, D. Schaefer, J. Loidl *et al.*, 2005 Partner choice during meiosis is regulated by Hop1-promoted dimerization of Mek1. *Mol Biol Cell* 16: 5804-5818.
- Niu, H., L. Wan, V. Busygina, Y. Kwon, J. A. Allen *et al.*, 2009 Regulation of meiotic recombination via Mek1-mediated Rad54 phosphorylation. *Mol Cell* 36: 393-404.
- Norris, D., and M. A. Osley, 1987 The two gene pairs encoding H2A and H2B play different roles in the *Saccharomyces cerevisiae* life cycle. *Mol. Cell Biol.* 7: 3473-3481.
- Oh, S. D., J. P. Lao, P. Y. Hwang, A. F. Taylor, G. R. Smith *et al.*, 2007 BLM ortholog, Sgs1, prevents aberrant crossing-over by suppressing formation of multichromatid joint molecules. *Cell* 130: 259-272.
- Ohta, K., T. Shibata and A. Nicolas, 1994 Changes in chromatin structure at recombination initiation sites during yeast meiosis. *Embo J* 13: 5754-5763.
- Pan, J., M. Sasaki, R. Kniewel, H. Murakami, H. G. Blitzblau *et al.*, 2011 A hierarchical combination of factors shapes the genome-wide topography of yeast meiotic recombination initiation. *Cell* 144: 719-731.
- Panizza, S., M. A. Mendoza, M. Berlinger, L. Huang, A. Nicolas *et al.*, 2011 Spo11-accessory proteins link double-strand break sites to the chromosome axis in early meiotic recombination. *Cell* 146: 372-383.
- Penedos, A., A. L. Johnson, E. Strong, A. S. Goldman, J. A. Carballo *et al.*, 2015 Essential and checkpoint functions of budding yeast ATM and ATR during meiotic prophase are facilitated by differential phosphorylation of a meiotic adaptor protein, Hop1. *PloS one* 10: e0134297.
- Perez-Hidalgo, L., S. Moreno and P. A. San-Segundo, 2003 Regulation of meiotic progression by the meiosis-specific checkpoint kinase Mek1 in fission yeast. *J Cell Sci* 116: 259-271.
- Preuss, U., G. Landsberg and K. H. Scheidtmann, 2003 Novel mitosis-specific phosphorylation of histone H3 at Thr11 mediated by Dlk/ZIP kinase. *Nucleic acids research* 31: 878-885.
- R Development Core Team, 2012 R: A language and environment for statistical computing, pp. R Foundation for Statistical Computing, Vienna, Austria.
- Rockmill, B., and G. S. Roeder, 1991 A meiosis-specific protein kinase homolog required for chromosome synapsis and recombination. *Genes Dev* 5: 2392-2404.
- Shimada, M., H. Niida, D. H. Zineldeen, H. Tagami, M. Tanaka *et al.*, 2008 Chk1 is a histone H3 threonine 11 kinase that regulates DNA damage-induced transcriptional repression. *Cell* 132: 221-232.
- Shinohara, A., H. Ogawa and T. Ogawa, 1992 Rad51 protein involved in repair and recombination in *S. cerevisiae* is a RecA-like protein. *Cell* 69: 457-470.

- Shroff, R., A. Arbel-Eden, D. Pilch, G. Ira, W. M. Bonner *et al.*, 2004 Distribution and dynamics of chromatin modification induced by a defined DNA double-strand break. *Curr Biol* 14: 1703-1711.
- Sikorski, R. S., and P. Hieter, 1989 A system of shuttle vectors and yeast host strains designed for efficient manipulation of DNA in *Saccharomyces cerevisiae*. *Genetics* 122: 19-27.
- Smith, A. V., and G. S. Roeder, 1997 The yeast Red1 protein localizes to the cores of meiotic chromosomes. *J Cell Biol* 136: 957-967.
- Sollier, J., W. Lin, C. Soustelle, K. Suhre, A. Nicolas *et al.*, 2004 Set1 is required for meiotic S-phase onset, double-strand break formation and middle gene expression. *EMBO J* 23: 1957-1967.
- Sommermeier, V., C. Beneut, E. Chaplais, M. E. Serrentino and V. Borde, 2013 Spp1, a member of the Set1 Complex, promotes meiotic DSB formation in promoters by tethering histone H3K4 methylation sites to chromosome axes. *Mol Cell* 49: 43-54.
- Subramanian, V. V., and A. Hochwagen, 2014 The meiotic checkpoint network: step-by-step through meiotic prophase. *Cold Spring Harbor perspectives in biology* 6: a016675.
- Subramanian, V. V., A. J. MacQueen, G. Vader, M. Shinohara, A. Sanchez *et al.*, 2016 Chromosome synapsis alleviates Mek1-dependent suppression of meiotic DNA repair. *PLoS Biol* 14: e1002369.
- Suhandynata, R. T., L. Wan, H. Zhou and N. M. Hollingsworth, 2016 Identification of putative Mek1 substrates during meiosis in *Saccharomyces cerevisiae* using quantitative phosphoproteomics. *PloS one* 11: e0155931.
- Sun, X., L. Huang, T. E. Markowitz, H. G. Blitzblau, D. Chen *et al.*, 2015 Transcription dynamically patterns the meiotic chromosome-axis interface. *eLife* 4.
- Thacker, D., N. Mohibullah, X. Zhu and S. Keeney, 2014 Homologue engagement controls meiotic DNA break number and distribution. *Nature* 510: 241-246.
- Tung, K. S., E. J. Hong and G. S. Roeder, 2000 The pachytene checkpoint prevents accumulation and phosphorylation of the meiosis-specific transcription factor Ndt80. *Proc Natl Acad Sci U S A* 97: 12187-12192.
- Usui, T., H. Ogawa and J. H. Petrini, 2001 A DNA damage response pathway controlled by Tel1 and the Mre11 complex. *Mol Cell* 7: 1255-1266.
- Wan, L., T. de los Santos, C. Zhang, K. Shokat and N. M. Hollingsworth, 2004 Mek1 kinase activity functions downstream of *RED1* in the regulation of meiotic double strand break repair in budding yeast. *Mol Biol Cell* 15: 11-23.

- Weiner, A., A. Hughes, M. Yassour, O. J. Rando and N. Friedman, 2010 High-resolution nucleosome mapping reveals transcription-dependent promoter packaging. *Genome Res* 20: 90-100.
- Wu, T.-C., and M. Lichten, 1994 Meiosis-induced double-strand break sites determined by yeast chromatin structure. *Science* 263: 515-518.
- Xu, L., M. Ajimura, R. Padmore, C. Klein and N. Kleckner, 1995 *NDT80*, a meiosis-specific gene required for exit from pachytene in *Saccharomyces cerevisiae*. *Molecular and cellular biology* 15: 6572-6581.
- Xu, L., B. M. Weiner and N. Kleckner, 1997 Meiotic cells monitor the status of the interhomolog recombination complex. *Genes Dev* 11: 106-118.
- Yang, W., Y. Xia, D. Hawke, X. Li, J. Liang *et al.*, 2012 PKM2 phosphorylates histone H3 and promotes gene transcription and tumorigenesis. *Cell* 150: 685-696.
- Zakharyevich, K., Y. Ma, S. Tang, P. Y. Hwang, S. Boiteux *et al.*, 2010 Temporally and biochemically distinct activities of Exo1 during meiosis: double-strand break resection and resolution of double Holliday junctions. *Mol Cell* 40: 1001-1015.
- Zhang, L., H. Ma and B. F. Pugh, 2011 Stable and dynamic nucleosome states during a meiotic developmental process. *Genome Res* 21: 875-884.
- Zickler, D., and N. Kleckner, 1999 Meiotic chromosomes: integrating structure and function. *Annu Rev Genet* 33: 603-754.
- Zickler, D., and N. Kleckner, 2015 Recombination, pairing, and synapsis of homologs during meiosis. *Cold Spring Harbor perspectives in biology* 7.

FIGURE LEGENDS

Figure 1. H3 T11 phosphorylation in *S. cerevisiae* meiosis.

(A) Western blots of whole-cell extracts from asynchronous cycling vegetative (Cyc) and synchronized meiotic culture time points in wild-type and mutant strains. In panels i–iv, the antibodies used were anti-H3 T11ph polyclonal (Active Motif 39151), anti-H3 S10ph monoclonal (EMD Millipore 05-817), anti-H2A S129ph/γ-H2A (Abcam 15083), and anti-H3 (Abcam 1791). For panels v and vi, anti-H3 T11ph monoclonal (EMD Millipore 05-789) and anti-H3 S10ph polyclonal (EMD Millipore 06-560) were used; other antibodies were the same. Interstitial lanes were removed from the blot images in panel vi to match time points in other panels. Filled and open arrowheads indicate 20 and 15 kDa molecular weight markers, respectively. (B) Western blot comparison of anti-H3 T11ph monoclonal (mAb; EMD Millipore 05-789) and polyclonal (pAb; Active Motif 39151) antibodies. (C) Meiotic progression assessed by DAPI staining. Cells with ≥ 2 DAPI-staining bodies were scored as having progressed past the first meiotic division; $n \geq 100$ cells per time point. The *rad50S* culture was not quantified past 6 hr because of nuclear fragmentation. (D) The first twenty amino acids in histone H3 and modifications known to occur in *S. cerevisiae* or *S. pombe*: ac, acetylation; me, methylation; ph, phosphorylation. (E) Meiosis-specificity of DNA damage-induced H3 T11ph. Asynchronous vegetative cultures of wild type were treated with genotoxins that induce DSBs, then whole-cell extracts were prepared and analyzed by western blotting for H3 T11ph. Cultures in the left panel were untreated (Mock) or treated with X-rays (400 Gy) or camptothecin (20 μM) at room temperature. An interstitial lane was deleted from the blot image for this panel. Cultures in the right panel were untreated or treated with X-rays (400 Gy) on ice. Premeiotic (0 hr) and meiotic (4 hr) cultures were included as controls. The anti-H3 T11ph monoclonal (EMD Millipore 05-789) was used. Arrowheads are as defined in panel A.

Figure 2. H3 T11 phosphorylation in *S. pombe* meiosis.

Western blots of whole-cell extracts from haploid *pat1-114* strains undergoing synchronized meiosis. Antibodies used were the same as in **Figure 1A**v. Filled and open arrowheads indicate 20 and 15 kDa molecular weight markers, respectively. The altered electrophoretic mobility of histones at later time points in some cultures was probably caused by varying levels of contaminating DNA in the extracts rather than differential post-translational modifications.

Figure 3. H3 T11 is a direct target of Mek1 kinase.

(A) Persistence of H3 T11ph requires maintenance of Mek1 kinase activity. A meiotic culture of a *mek1-as, dmc1Δ* (strain SKY3095) was split 4 hr after transfer to sporulation medium. One part was left to continue in meiosis untreated, the other part was treated with 1 μM 1-NA-PP1. Whole-cell extracts were prepared at the indicated times and assayed for H3 T11ph by western blotting (mAb; EMD Millipore 05-789). Filled and open arrowheads indicate 20 and 15 kDa molecular weight markers, respectively. Numbers indicate hours after transfer to sporulation medium. (B) Mek1 kinase assay using radioactive ATP. Affinity-purified GST-Mek1 (250 ng) was incubated in the presence of [γ - 32 P]ATP either alone or with 2 μg recombinant H3 or 5 μg of unphosphorylated or phosphorylated synthetic H3 1-20 peptides as substrates. Reactions were separated by SDS-PAGE and visualized by autoradiography (top), anti-H3 T11ph western blot (middle; polyclonal Active Motif 39151), and Coomassie staining. (C) Mek1 kinase assay by semisynthetic epitope labeling. Kinase reactions were carried out with affinity-purified GST-Mek1 (2 μg) or GST-Mek1-as (0.76 μg) in the presence of ATPγS or 6-Fu-ATPγS with 2 μg recombinant H3. After incubation 30 min at 30°C, PNBm (*p*-nitrobenzyl mesylate) was added to alkylate the thiophosphorylated target sites. Reactions were then separated by SDS-PAGE and analyzed by western blotting with anti-thiophosphate ester monoclonal antibody (top panel;

Epitomics 2686-1) or anti-H3 T11ph monoclonal antibody (EMD Millipore 05-789). Interstitial lanes were removed from images in panels B and C as indicated by the white lines.

Figure 4. Characterization of histone mutant strains.

(A) Composite of western blots of whole-cell extracts from synchronous meiotic cultures or asynchronous cycling vegetative cultures (“C”) carrying the indicated histone mutations. Antibodies used were: anti-H3 T11ph polyclonal (Active Motif 39151) or anti-H3 T11ph monoclonal (EMD Millipore 05-789); anti-H3 S10ph monoclonal (EMD Millipore 05-817); anti-H3 S10ph polyclonal (EMD Millipore 06-560); anti- γ -H2A (Abcam 15083); and anti-H3 (Abcam 1791). Filled and open arrowheads indicate 20 and 15 kDa molecular weight markers, respectively. “n.d.” indicates not determined; “*hht2-ΔN*” encodes H3 lacking its N-terminal 30 amino acids. (B) Vegetative growth of H3 mutant strains. Cells from overnight cultures were spotted onto YPD plates using a manifold pin replicator and represent 1:5 serial dilutions starting with $\sim 2.5 \times 10^6$ cells/ml. (C) Analysis of meiotic DSB formation. High-molecular-weight DNA isolated in agarose plugs was separated by pulsed-field gel electrophoresis followed by Southern blotting and indirect end-labeling with a probe directed against *CHAI* on the left arm of chromosome III. The lower panel shows quantification of the DSB signal as percent of lane total after background subtraction. (D,E) Meiotic progression of representative histone mutant strains. Cells were fixed and stained with DAPI and the fraction of cells with ≥ 2 nuclei was counted ($n \geq 100$ cells per time point). For panel E, strains used were *rad51Δ* (SKY3183); *rad51Δ*, *H3 S10A*, *T11V* (SKY3186); *dmc1Δ*, *rad54 T132A* (SKY3802); *dmc1Δ*, *rad54 T132A*, *H3 T11V* (SKY3659); *dmc1Δ* (SKY3078) and; *dmc1Δ* *H3 S10A*, *T11V* (SKY3091). (F) Spore viabilities in plasmid shuffle strains expressing wild-type H3 or H3 T11A. Three independent clones isolated for each genotype were sporulated and tetrads were dissected in three separate experiments. Each point represents the value from a single isolate ($n = 30$ –32 tetrads per data point). See **Table 1** for summary and text for statistical test. Strains used were: H3 wild type (SKY3438-3440) and *H3 T11A* (SKY3441-3443). (G) Evidence that the *H3 T11V* mutation increases MI nondisjunction in a *rad54-T132A dmc1Δ* background. The distribution of viable spores in tetrads is shown for the indicated strains. An increase in 2- and 0-spore-viable tetrads (rather than 3- or 1-spore-viable) is diagnostic of an increased frequency of MI nondisjunction. Strains were *dmc1Δ*, *rad54 T132A* (SKY3802) and *dmc1Δ*, *rad54 T132A*, *H3 T11V* (SKY3659).

Figure 5. Spatial disposition of H3 T11ph along meiotic chromosomes.

(A,B) Anti-H3 and anti-H3 T11ph ChIP-seq coverage across representative genomic regions. Coverage data for each chromosome were normalized to chromosome mean and \log_2 -transformed. Green trace shows the difference between the H3 and H3 T11ph traces, i.e., the phosphorylation-specific signal. The Spo11-oligo map (RPM, reads per million) (Mohibullah and Keeney 2016) and decile-normalized anti-Red1 ChIP-chip data (Panizza *et al.* 2011) are shown for comparison. All ChIP data were smoothed with a 500-bp Parzen (triangular) moving average. Color coding is retained in the other panels in this figure. (C) H3 T11ph enrichment around presumed axis-attachment sites. H3 and H3 T11ph ChIP-seq coverage (upper graph) and smoothed (500-bp Parzen window) Red1 and Hop1 ChIP-chip data (lower graph, Panizza *et al.* 2011) were averaged around 849 Red1 ChIP peaks. (D) H3 T11ph correlates well with Red1 and Hop1 ChIP signal genome wide. Each point compares the H3 or H3 T11ph ChIP-seq coverage with Red1 or Hop1 ChIP-chip signal averaged across non-overlapping 5-kb bins. Correlation coefficients (Pearson’s *r*) are indicated in each plot. (E) H3 T11ph around DSB hotspots. ChIP-seq and Spo11-oligo data were averaged around 3908 Spo11-oligo hotspots (Mohibullah and Keeney 2016). Note that vertical and horizontal scales for ChIP-seq data are the same in panels C and E to facilitate direct comparison. Inset shows higher magnification view of patterns in the

immediate vicinity of hotspots. **(F–I)** Correlation between anti-H3, anti-H3 T11ph, and difference (Δ) maps to binding of the indicated proteins, binned in non-overlapping windows of varying size.

SUPPLEMENTAL FIGURE LEGENDS

Supplemental Figure S1. Specificity of anti-H3 T11ph and anti-H3 S10ph antibodies.

(A) Histone peptide array western blots showing the specificity of (i) anti-H3 T11ph mAb or (ii) anti-H3 S10ph pAb and their tolerance of neighboring modifications. Blots are of duplicate 384-peptide arrays (MODified Histone Peptide Array, Active Motif 13001) of immobilized synthetic histone H2A, H2B, H3 and H4 unmodified peptides or peptides containing from one to four modified residues including many possible combinations of histone modifications that are found in higher eukaryotes, of which only a small number are known to be present in yeast. Positions A1–L11 contain H3 peptides, L12–O11 contain H4 peptides, O12–P3 contain H2A peptides and P4–P19 contain H2B peptides. Peptides that were highly reactive with either antibody are listed below the blot image; the entire table of peptides is listed in **Supplemental Table S2**. (B) Immunodetection of histone H3 amino-terminal peptides (residues 1–20) or recombinant histone proteins spotted onto PVDF membranes demonstrating the specificity of antibodies to phospho-H3 T11 and phospho-H3 S10. Spots were 10-fold serial dilutions of peptides or recombinant histones starting with 167 ng in the left-most column. Recombinant histone proteins produced in *E. coli* were from the following species: H2A, H2B, H3 from *S. cerevisiae*; H3.3 from *H. sapiens*; and H4 from *X. laevis*. Antibodies were: anti-H3 pAb (Abcam 1791), which is specific to the carboxy-terminal 35 amino acids of histone H3; anti-H3 T11ph polyclonal (Active Motif 39151); anti-H3 S10ph monoclonal (EMD Millipore 05-817); and anti-H3 S10ph polyclonal (EMD Millipore 06-560).

Notes:

(Panel Ai) The diphosphorylated H3 1–19 S10ph T11ph peptide at position D5 was not detected by the anti-H3 T11ph mAb, whereas all phospho-T11 containing peptides (except those that also contained phospho-S10) were detected (peptides containing phospho-T11 along with methyl-K4 were not included in the array). We conclude that this mAb detects only the monophosphorylated peptide, but that it is tolerant of other modifications of the H3 N-terminal tail.

(Panel Aii) The diphosphorylated (S10ph T11ph) peptide at position D5 was not detected by the anti-H3 S10ph pAb, whereas all phospho-S10 containing peptides (except those that also contained phospho-T11) were detected (peptides containing phospho-S10 along with methyl-K4 were not included in the array). We conclude that this pAb detects only the monophosphorylated peptide, but that it is relatively tolerant of other modifications of the H3 N-terminal tail. This pAb showed detectable cross-reaction to other modifications as well. Peptides that scored as weakly reactive with anti-H3 S10ph pAb were: J6, H3 1–19 S10ph K14ac; J11, H3 7–26 K18ac; J13, H3 7–26 K14ac R17me2s; J15, H3 7–26 R17me2s K18ac; J19, H3 7–26 K14ac R17me2a K18ac; K4, H3 16–35 S28ph; L7, H3 26–45 unmodified; L8, H3 26–45 K36me1; L9, H3 26–45 K36me2; L11, H3 26–45 K36ac; M18, H4 11–30 unmodified; M19, H4 11–30 K12ac; M20, H4 11–30 K16ac; M21, H4 11–30 R17me2s; M22, H4 11–30 R17me2a; N5, H4 11–30 R24me2a; N6, H4 11–30 R24me2s; N7, H4 11–30 K12ac K16ac; N8, H4 11–30 K16ac R17me2s; N9, H4 11–30 K16ac R17me2a.

(Panel B) Anti-H3 T11ph pAb was capable of detecting phospho-T11 even with nearby methylation at lysine 9, a modification that occurs in *S. pombe* and metazoans, but not in *S. cerevisiae*. Both anti-H3 S10ph antibodies also reacted slightly with full-length recombinant H3 and H3.3.

Table 1. Absence of H3 T11ph does not compromise spore viability.

Mutation method ^a	H3 genotype ^b	Strain	Spore viability (no. of tetrads)
Replacement	Wild type	2701	97% (44)
	<i>S10A T11V</i>	2705	97% (44)
H3-H4 integration	Wild type	3311	96% (22)
	<i>S10A</i>	3333	97% (64)
	<i>T11V</i>	3342	95% (64)
	<i>S10A T11V</i>	3334	93% (64)
	<i>T11A</i>	3312	95% (86)
	<i>T11S</i>	3313	99% (22)
	<i>T11D</i>	3332	97% (64)
	<i>T11E</i>	3303	97% (64)
Four-core integration	Wild type	3330	94% (22)
	<i>T11V</i>	3264	97% (64)
	ΔN	2388	81% (44)
Plasmid shuffle, Expt. 1 ^c	Wild type	3438–3440	90% (90)
	<i>T11A</i>	3441–3443	86% (90)
Plasmid shuffle, Expt. 2 ^c	Wild type	3438–3440	75% (92)
	<i>T11A</i>	3441–3443	77% (94)
Plasmid shuffle, Expt. 3 ^c	Wild type	3438–3440	74% (96)
	<i>T11A</i>	3441–3443	76% (96)

^a Replacement: Both *HHT1* and *HHT2* were replaced with wild-type or mutant copies at their endogenous locations. Integration: Stable integration at *leu2::hisG* of a cassette carrying either the H3 and H4 gene pair *HHT2-HHF2*, or all four core histone genes *HTA1-HTB1* and *HHT2-HHF2*. Endogenous loci (encoding H3 and H4 or all four core histones, respectively) were deleted. Plasmid shuffle: Replacement of a *URA3* plasmid carrying wild-type *HHT2-HHF2* with a *LEU2* plasmid carrying either wild-type or mutant versions. The endogenous H3 and H4 loci were deleted.

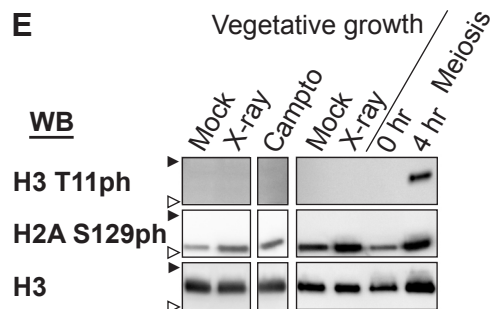
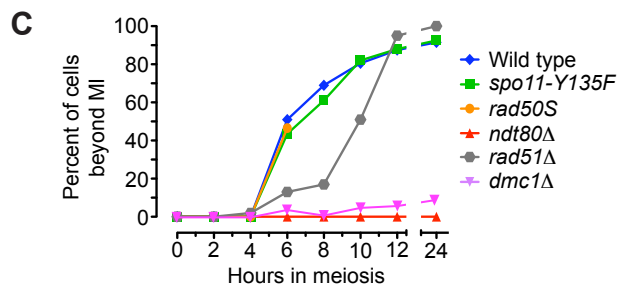
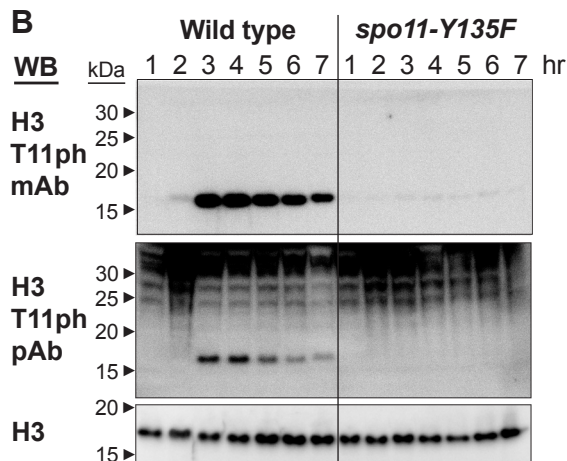
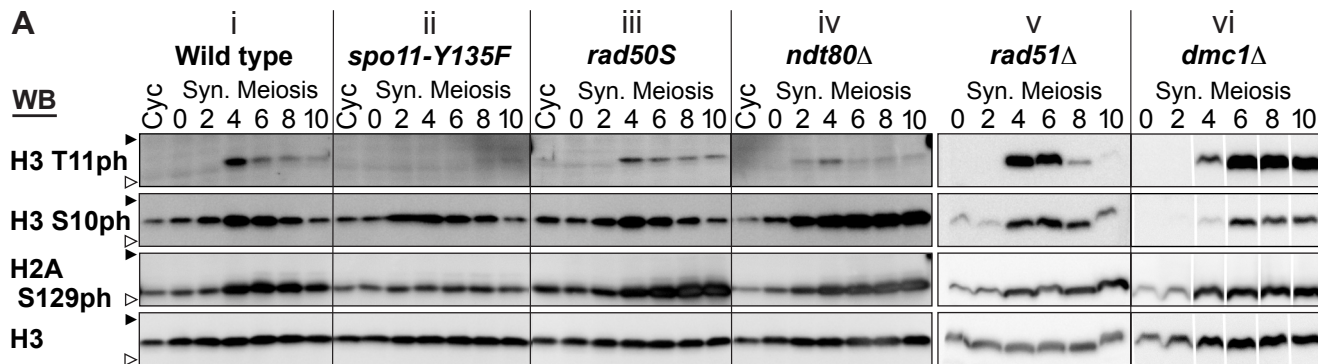
^b Genotypes are homozygous unless plasmid-based. See **Supplemental Table S1** for complete genotypes.

^c Three independent 5-FOA^R colonies were isolated for each shuffle plasmid and were dissected separately. The dissections were performed on three separate occasions by two different investigators; all six strains were dissected in parallel in each experiment. A breakdown of results by strain and experiment is provided in **Figure 4F**. Neither histone H3 genotype nor clone identity was a significant predictor of altered spore viability ($p \geq 0.9$, linear regression).

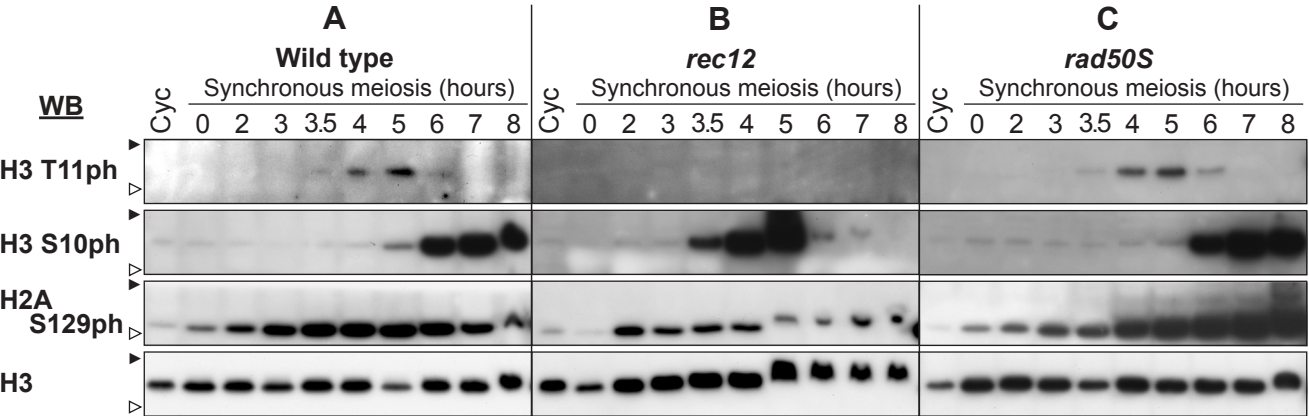
Table 2. Combining *H3 T11* mutations with other mutations.

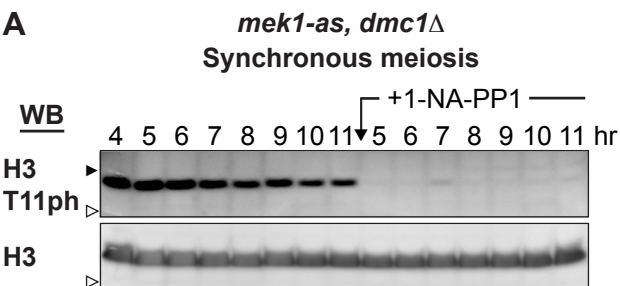
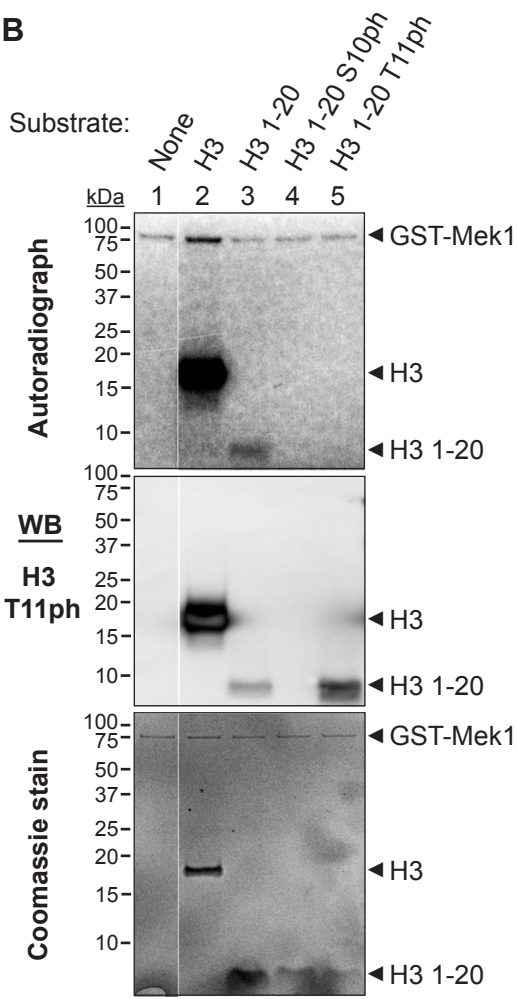
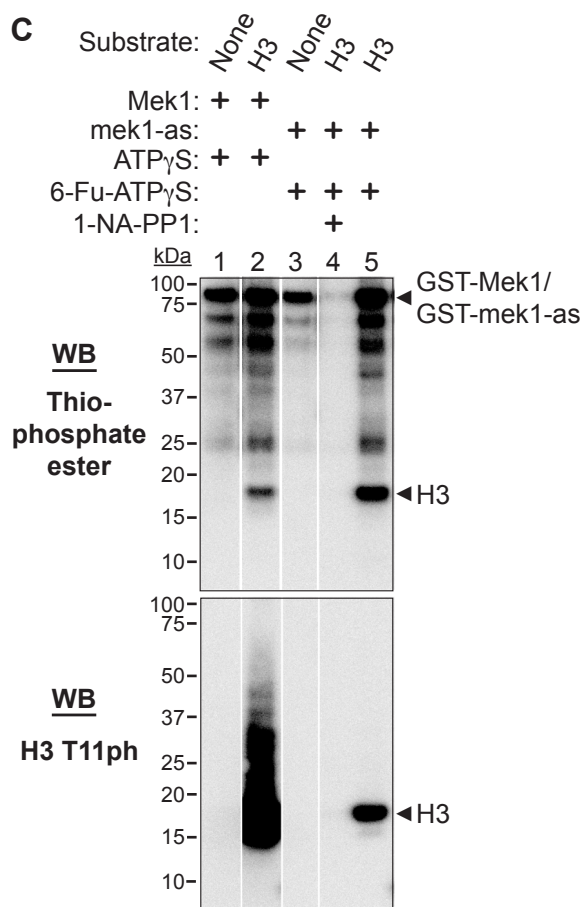
Additional mutation(s)^a	H3 genotype^a	Strain	Spore viability (no. of tetrads)
<i>H2A S129A</i>	wild type	3265	97% (64)
	<i>T11V</i>	3331	95% (64)
<i>set1Δ</i>	wild type	4415	97% (42)
	<i>S10A T11V</i>	3329	97% (64)
<i>rad51Δ</i>	wild type	3183	0% (44)
	<i>S10A T11V</i>	3186	0% (44)
<i>rad54-T132A dmc1Δ</i>	wild type	3802	67% (65)
	<i>T11V</i>	3659	49% (86)

^a Genotypes are homozygous. See **Supplemental Table S1** for complete genotypes.

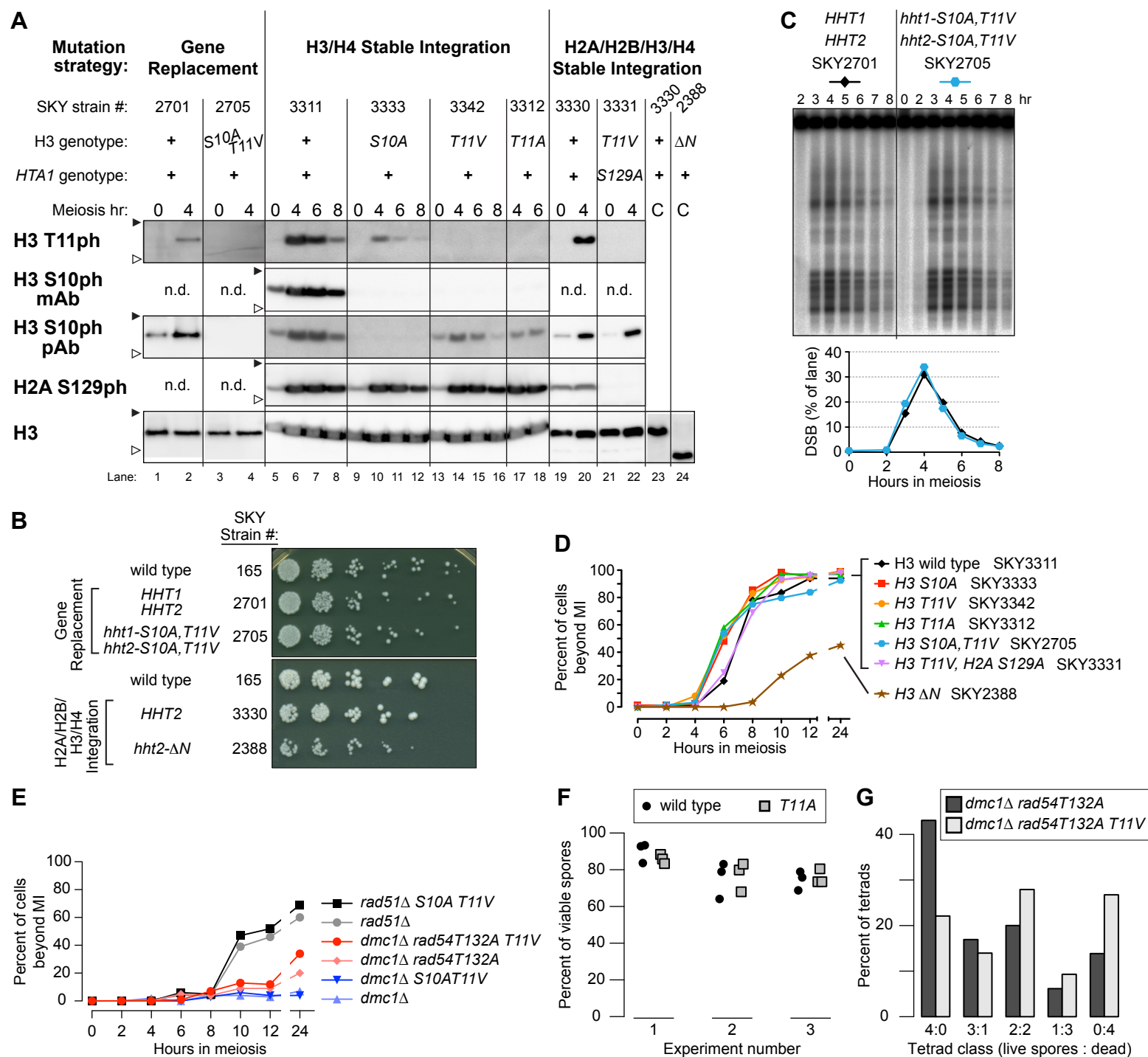


Kniewel et al., Figure 2

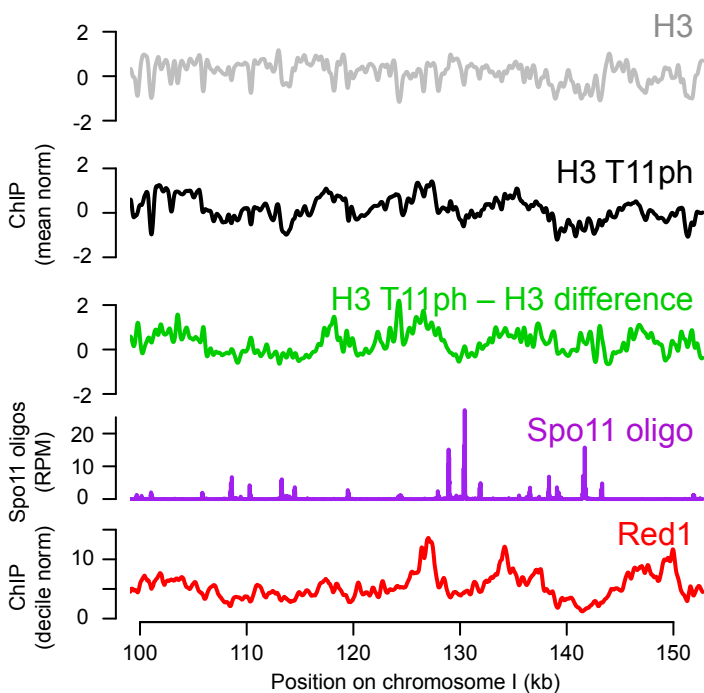


A**B****C**

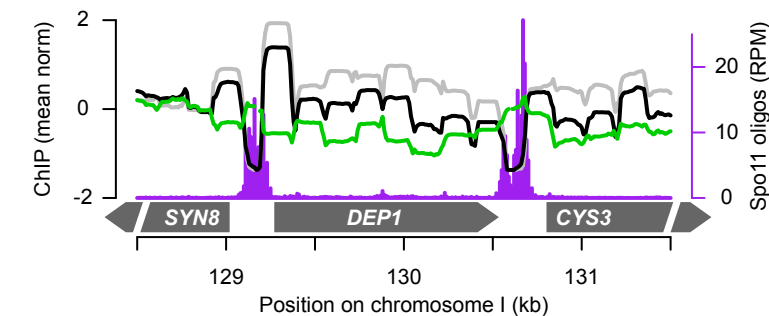
Kniewel et al., Figure 4



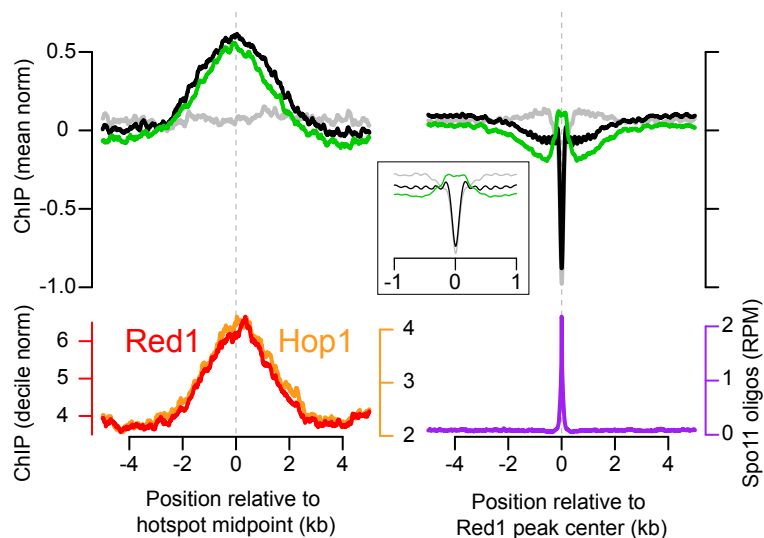
A



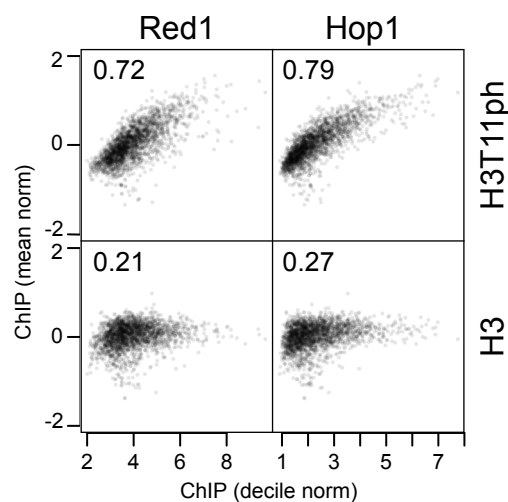
B



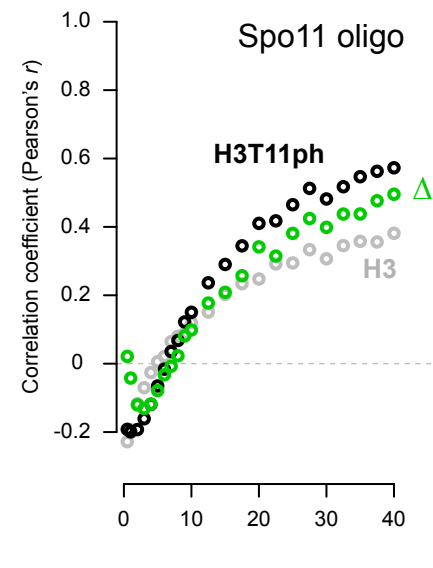
C



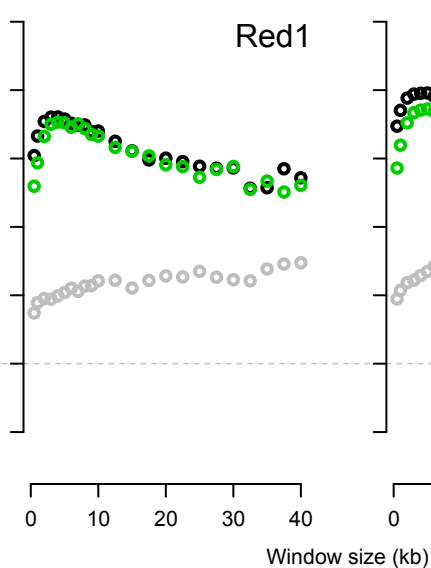
D



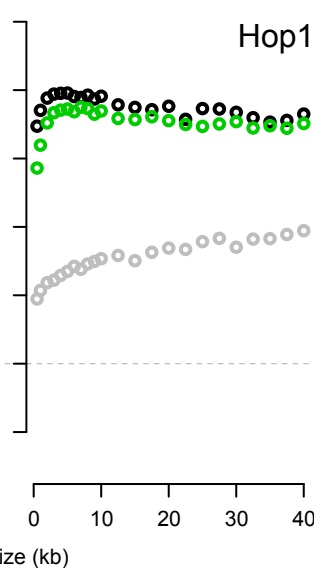
F



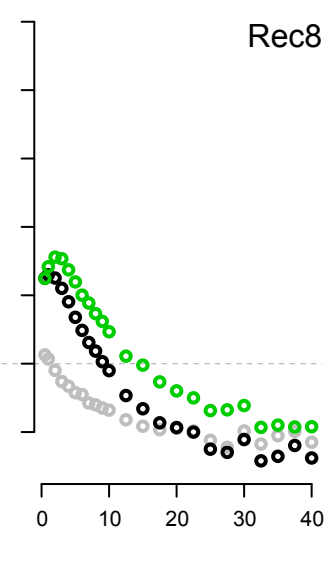
G

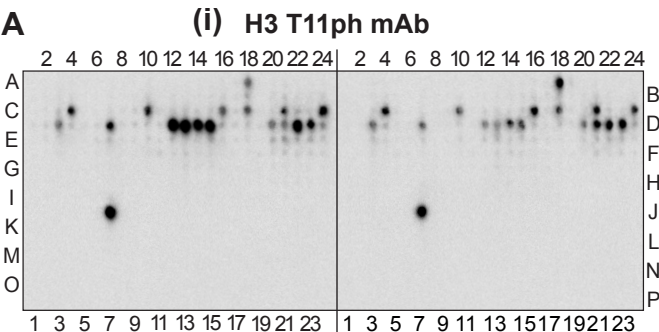


H



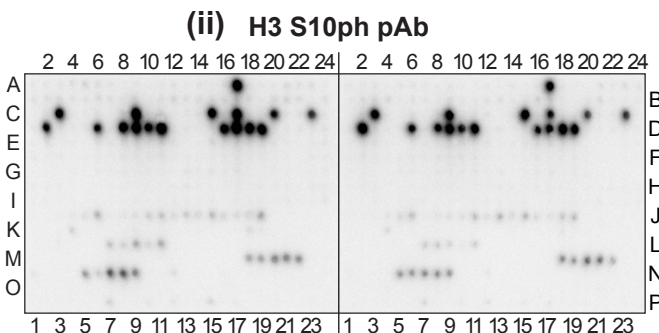
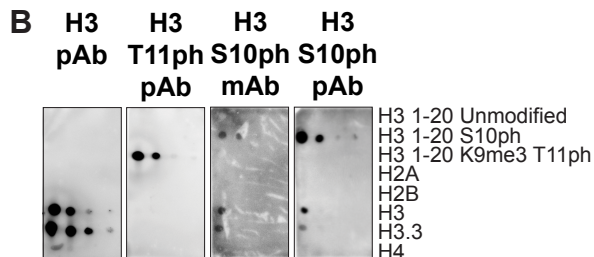
I





Highly Positive Peptides:

A18 H3 1-19 T11ph	D12 H3 1-19 R8me2s K9me1 T11ph
C4 H3 1-19 R8me2s T11ph	D13 H3 1-19 R8me2s K9me2 T11ph
C10 H3 1-19 R8me2a T11ph	D14 H3 1-19 R8me2s K9me2 T11ph
C16 H3 1-19 R8cit T11ph	D15 H3 1-19 R8me2s K9ac T11ph
C18 H3 1-19 K9me1 T11ph	D20 H3 1-19 R8me2a K9me1 T11ph
C21 H3 1-19 K9me2 T11ph	D21 H3 1-19 R8me2a K9me2 T11ph
C24 H3 1-19 K9me3 T11ph	D22 H3 1-19 R8me2a K9me3 T11ph
D3 H3 1-19 K9ac T11ph	D23 H3 1-19 R8me2s K9ac T11ph
D7 H3 1-19 T11ph K14ac	J7 H3 7-26 T11ph K14ac



Highly Positive Peptides:

A17 H3 1-19 S10ph	D8 H3 1-19 R8me2s K9me1 S10ph
C3 H3 1-19 R8me2s S10ph	D9 H3 1-19 R8me2s K9me2 S10ph
C9 H3 1-19 R8me2a S10ph	D10 H3 1-19 R8me2s K9me2 S10ph
C15 H3 1-19 R8cit S10ph	D11 H3 1-19 R8me2s K9ac S10ph
C17 H3 1-19 K9me1 S10ph	D16 H3 1-19 R8me2a K9me1 S10ph
C20 H3 1-19 K9me2 S10ph	D17 H3 1-19 R8me2a K9me2 S10ph
C23 H3 1-19 K9me3 S10ph	D18 H3 1-19 R8me2a K9me3 S10ph
D2 H3 1-19 K9ac S10ph	D19 H3 1-19 R8me2s K9ac S10ph
D6 H3 1-19 S10ph K14ac	

Supplemental Table S1. List of *S. cerevisiae* and *S. pombe* strains used in this study.

<i>S. cerevisiae</i>, SK1 background^a		
Strain SKY#	Genotype	Reference or source
Strains for Figure 1: Genetic requirements of H3 T11ph		
165 ^a		(CHA <i>et al.</i> 2000)
198	<i>HO, lys2, ura3::hisG, spo11-Y135F-HA::URA</i>	(CHA <i>et al.</i> 2000)
50	<i>leu2, arg4-Nsp, nuc1Δ::LEU2, rad50-K81I (rad50S)::URA3</i>	(LIU <i>et al.</i> 1995)
2051	<i>ndt80Δ::LEU2</i>	(XU <i>et al.</i> 1995)
3455	<i>ho::hisG, ura3(Δ<i>sma-pst</i>), rad51Δ::hisG-URA3-hisG</i>	Neil Hunter
2578	<i>his4-X, dmc1Δ::LEU2</i>	(BISHOP <i>et al.</i> 1992)
Strain for Figure 3: H3 T11ph kinase determination		
3095	<i>his4-X/his4-B, ura3::GST-mek1-as1::URA3/ura3, mek1Δ::kanMX6, dmc1Δ::LEU2</i>	(WAN <i>et al.</i> 2004)
Strains for Table 1, Table 2 and Figure 4: H3 T11 mutants		
2701	<i>HHT1::kanMX4, HHT2::hphMX4</i>	This study
2705	<i>hht1-S10A, T11V::kanMX4; hht2-S10A, T11V::hphMX4</i>	This study
3166	<i>MATa, ho::LYS2, lys2, leu2::hisG, ura3, hht1-hhf1Δ::kanMX, hhf2-hht2Δ::natMX, hta2-htb2Δ::natMX, pRK12[CEN6/ARS4, URA3, HTA1-HTB1, HHF2-HHT2]</i>	This study
3167	<i>MATα, ho::LYS2, lys2, leu2::hisG, ura3, hht1-hhf1Δ::kanMX, hhf2-hht2Δ::natMX, hta2-htb2Δ::natMX, pRK12[CEN6/ARS4, URA3, HTA1-HTB1, HHF2-HHT2]</i>	This study
3311	<i>hht1-hhf1Δ::kanMX, hhf2-hht2Δ::natMX, hta2-htb2Δ::natMX, leu2::HHF2-HHT2::LEU2</i>	This study
3333	<i>hht1-hhf1Δ::kanMX, hhf2-hht2Δ::natMX, hta2-htb2Δ::natMX, leu2::HHF2-hht2-S10A::LEU2</i>	This study
3342	<i>hht1-hhf1Δ::kanMX, hhf2-hht2Δ::natMX, hta2-htb2Δ::natMX, leu2::HHF2-hht2-T11V::LEU2</i>	This study
3334	<i>hht1-hhf1Δ::kanMX, hhf2-hht2Δ::natMX, hta2-htb2Δ::natMX; leu2::HHF2-hht2-S10A, T11V::LEU2</i>	This study
3312	<i>hht1-hhf1Δ::kanMX, hhf2-hht2Δ::natMX, hta2-htb2Δ::natMX, leu2::HHF2-hht2-T11A::LEU2</i>	This study
3313	<i>hht1-hhf1Δ::kanMX, hhf2-hht2Δ::natMX, hta2-htb2Δ::natMX, leu2::HHF2-hht2-T11S::LEU2</i>	This study

Supplemental Table 1 (continued).

3332	<i>hht1-hhf1Δ::kanMX, hhf2-hht2Δ::natMX, hta2-htb2Δ::natMX, leu2::HHF2-hht2-T11D::LEU2</i>	This study
3303	<i>hht1-hhf1Δ::kanMX, hhf2-hht2Δ::natMX, hta2-htb2Δ::natMX, leu2::HHF2-hht2-T11E::LEU2</i>	This study
2283	<i>hht1-hhf1Δ::kanMX, hhf2-hht2Δ::natMX, hta2-htb2Δ::natMX, hta1-htb1Δ::hphMX, pRK12[CEN6/ARS4, URA3, HTA1-HTB1, HHF2-HHT2]</i>	This study
3330	<i>hht1-hhf1Δ::kanMX, hhf2-hht2Δ::natMX, hta2-htb2Δ::natMX, hta1-htb1Δ::hphMX, leu2::HTA1-HTB1-HHF2-HHT2-LEU2</i>	This study
3264	<i>hht1-hhf1Δ::kanMX, hhf2-hht2Δ::natMX, hta2-htb2Δ::natMX, hta1-htb1Δ::hphMX, leu2::HTA1-HTB1-HHF2-hht2-T11V::LEU2</i>	This study
2388	<i>hht1-hhf1Δ::kanMX, hhf2-hht2Δ::natMX, hta2-htb2Δ::natMX, hta1-htb1Δ::hphMX, leu2::HTA1-HTB1-HHF2-hht2-Δ1-30(ΔN)::LEU2</i>	This study
3428	<i>hht1-hhf1Δ::kanMX, hhf2-hht2Δ::natMX, hta2-htb2Δ::natMX, leu2::HHF2-HHT2::LEU2, arg4-Nsp/arg4-Bgl</i>	This study & (MARTINI <i>et al.</i> 2006)
3431	<i>hht1-hhf1Δ::kanMX, hhf2-hht2Δ::natMX, hta2-htb2Δ::natMX, leu2::HHF2-hht2-T11A::LEU2, arg4-Nsp/arg4-Bgl</i>	This study & (MARTINI <i>et al.</i> 2006)
3438, 3439, 3440 ^b	<i>trp1::hisG, his4-N/his4-G, hhf1-hht1Δ::LEU2, hhf2-hht2Δ::trp1::kanMX3, pRK92[CEN, ARS, TRP1, HHT2-HHF2]</i>	(GOVIN <i>et al.</i> 2010)
3441, 3442, 3443 ^b	<i>trp1::hisG, his4-N/his4-G, hhf1-hht1Δ::LEU2, hhf2-hht2Δ::trp1::kanMX3, pRK93[CEN, ARS, TRP1, hht2-T11A-HHF2]</i>	(GOVIN <i>et al.</i> 2010)
3265	<i>hht1-hhf1Δ::kanMX, hhf2-hht2Δ::natMX, hta2-htb2Δ::natMX, hta1-htb1Δ::hphMX, leu2::hta1-S129A-HTB1-HHT2-HHF2::LEU2</i>	This study
3331	<i>hht1-hhf1Δ::kanMX, hhf2-hht2Δ::natMX, hta2-htb2Δ::natMX, hta1-htb1Δ::hphMX, leu2::hta1-S129A-HTB1-HHF2-hht2-T11V::LEU2</i>	This study
4415	<i>leu2::hisG or leu2-K, arg4-nsp, bgl or ARG4, HHT1::kanMX4, HHT2::hphMX4, set1Δ::kanMX</i>	This study & ORT4784 X ORT 4785 (SOLLIER <i>et al.</i>

		2004)
3329	<i>leu2::hisG</i> or <i>leu2-K</i> , <i>arg4-nsp</i> , <i>bgl</i> or <i>ARG4</i> , <i>hht1-S10A</i> , <i>T11V::kanMX4</i> , <i>hht2-S10A</i> , <i>T11V::hphMX4</i> , <i>set1Δ::kanMX</i>	This study
3183	<i>HHT1::kanMX/</i> ”, <i>HHT2::hygMX/</i> ”, <i>rad51Δ::hisG-URA3-hisG/</i> ”	This study
3186	<i>hht1-S10AT11V::kanMX/</i> ”, <i>hht2-S10AT11V::hygMX/</i> ”, <i>rad51Δ::hisG-URA3-hisG/</i> ”	This study
3802	<i>his4X</i> , <i>ura3::RAD54-T132A::URA3</i> , <i>dmc1Δ::hphMX4</i> , <i>rad54::kanMX6</i>	(NIU <i>et al.</i> 2009)
3659	<i>HIS4</i> , <i>ura3::RAD54-T132A::URA3</i> , <i>dmc1Δ::hphMX4</i> , <i>rad54::kanMX6</i> , <i>hht1-hhf1Δ::kanMX</i> , <i>hhf2-hht2Δ::natMX</i> , <i>hta2-htb2Δ::natMX</i> , <i>leu2::HHF2-hht2-T11V::LEU2</i>	This study
3078	<i>HHT1::kanMX4</i> , <i>HHT2::hphMX4</i> , <i>dmc1Δ::LEU2</i>	This study
3091	<i>hht1-S10A</i> , <i>T11V::kanMX4</i> , <i>hht2-S10A</i> , <i>T11V::hphMX4</i> , <i>dmc1Δ::LEU2</i>	This study

Strains for Figure 2: <i>S. pombe</i>, Standard background		
2594	<i>h+</i> , <i>pat1-114</i> , <i>ade6-3049</i>	(STEINER AND SMITH 2005)
2595	<i>h+</i> , <i>pat1-114</i> , <i>ade6-3049</i> , <i>rad50-K81I (rad50S)</i>	(YOUNG <i>et al.</i> 2002)
2596	<i>h-</i> , <i>pat1-114</i> , <i>ade6-3049</i> , <i>ura4-DIB</i> , <i>rec12-171::ura4⁺</i>	(DAVIS AND SMITH 2003)

^a All *S. cerevisiae* strains are diploid *MAT a/MAT α*, *ho::LYS2/*”, *lys2/*”, *leu2::hisG/*”, *ura3/*” (except SKY3166 and SKY3167) and homozygous at all loci unless otherwise noted (KANE AND ROTH 1974).

^b Three independent plasmid shuffle transformants.

Supplemental Table 2. Synthetic peptide array.

		Active Motif		MODified™ Histone Peptide Array*						
				Catalog Nos. 13001 & 13005						
Modification number	Peptide location	Peptide sequence			name	Mod1	Mod2	Mod 3	Mod 4	N-terminus
1	A 1	ARTKQTARKSTGGKAPRKQ			H3 1-19	unmod				free
2	A 2	ARme2sTKQTARKSTGGKAPRKQ			H3 1-19	R2me2s				free
3	A 3	ARme2aTKQTARKSTGGKAPRKQ			H3 1-19	R2me2a				free
4	A 4	ACitTKQTARKSTGGKAPRKQ			H3 1-19	R2Citr				free
5	A 5	ARpTKQTARKSTGGKAPRKQ			H3 1-19	T3P				free
6	A 6	ARTKme1QTARKSTGGKAPRKQ			H3 1-19	K4me1				free
7	A 7	ARTKme2QTARKSTGGKAPRKQ			H3 1-19	K4me2				free
8	A 8	ARTKme3QTARKSTGGKAPRKQ			H3 1-19	K4me3				free
9	A 9	ARTKacQTARKSTGGKAPRKQ			H3 1-19	K4ac				free
10	A10	ARTKQTARme2sKSTGGKAPRKQ			H3 1-19	R8me2s				free
11	A11	ARTKQTARme2aKSTGGKAPRKQ			H3 1-19	R8me2a				free
12	A12	ARTKQTACitKSTGGKAPRKQ			H3 1-19	R8Citr				free
13	A13	ARTKQTARKme1STGGKAPRKQ			H3 1-19	K9me				free
14	A14	ARTKQTARKme2STGGKAPRKQ			H3 1-19	K9m2				free
15	A15	ARTKQTARKme3STGGKAPRKQ			H3 1-19	K9me3				free
16	A16	ARTKQTARKacSTGGKAPRKQ			H3 1-19	K9ac				free
17	A17	ARTKQTARKpSTGGKAPRKQ			H3 1-19	S10P				free
18	A18	ARTKQTARKSpTGGKAPRKQ			H3 1-19	T11P				free
19	A19	ARTKQTARKSTGGKacAPRKQ			H3 1-19	K14ac				free
20	A20	ARme2spTKQTARKSTGGKAPRKQ			H3 1-19	R2me2s	T3P			free
21	A21	ARme2sTKme1QTARKSTGGKAPRKQ			H3 1-19	R2me2s	K4me1			free
22	A22	ARme2sTKme2QTARKSTGGKAPRKQ			H3 1-19	R2me2s	K4me2			free
23	A23	ARme2sTKme3QTARKSTGGKAPRKQ			H3 1-19	R2me2s	K4me3			free
24	A24	ARme2sTKacQTARKSTGGKAPRKQ			H3 1-19	R2me2s	K4ac			free
25	B 1	ARme2apTKQTARKSTGGKAPRKQ			H3 1-19	R2me2a	T3P			free
26	B 2	ARme2aTKme1QTARKSTGGKAPRKQ			H3 1-19	R2me2a	K4me1			free
27	B 3	ARme2aTKme2QTARKSTGGKAPRKQ			H3 1-19	R2me2a	K4me2			free
28	B 4	ARme2aTKme3QTARKSTGGKAPRKQ			H3 1-19	R2me2a	K4me3			free
29	B 5	ARme2aTKacQTARKSTGGKAPRKQ			H3 1-19	R2me2a	K4ac			free
30	B 6	ACitpTKQTARKSTGGKAPRKQ			H3 1-19	R2Citr	T3P			free
31	B 7	ACitTKme1QTARKSTGGKAPRKQ			H3 1-19	R2Citr	K4me1			free
32	B 8	ACitTKme2QTARKSTGGKAPRKQ			H3 1-19	R2Citr	K4me2			free
33	B 9	ACitTKme3QTARKSTGGKAPRKQ			H3 1-19	R2Citr	K4me3			free
34	B10	ACitTKacQTARKSTGGKAPRKQ			H3 1-19	R2Citr	K4ac			free
35	B11	ARpTKme1QTARKSTGGKAPRKQ			H3 1-19	T3P	K4me1			free
36	B12	ARpTKme2QTARKSTGGKAPRKQ			H3 1-19	T3P	K4me2			free
37	B13	ARpTKme3QTARKSTGGKAPRKQ			H3 1-19	T3P	K4me3			free
38	B14	ARpTKacQTARKSTGGKAPRKQ			H3 1-19	T3P	K4ac			free
39	B15	ARme2spTKme1QTARKSTGGKAPRKQ			H3 1-19	R2me2s	T3P	K4me1		free
40	B16	ARme2spTKme2QTARKSTGGKAPRKQ			H3 1-19	R2me2s	T3P	K4me2		free
41	B17	ARme2spTKme3QTARKSTGGKAPRKQ			H3 1-19	R2me2s	T3P	K4me3		free
42	B18	ARme2spTKacQTARKSTGGKAPRKQ			H3 1-19	R2me2s	T3P	K4ac		free
43	B19	ARme2apTKme1QTARKSTGGKAPRKQ			H3 1-19	R2me2a	T3P	K4me1		free
44	B20	ARme2apTKme2QTARKSTGGKAPRKQ			H3 1-19	R2me2a	T3P	K4me2		free
45	B21	ARme2apTKme3QTARKSTGGKAPRKQ			H3 1-19	R2me2a	T3P	K4me3		free
46	B22	ARme2apTKacQTARKSTGGKAPRKQ			H3 1-19	R2me2a	T3P	K4ac		free
47	B23	ARTKQTARme2aKme1STGGKAPRKQ			H3 1-19	R8me2s	K9me			free
48	B24	ARTKQTARme2aKme2STGGKAPRKQ			H3 1-19	R8me2s	K9m2			free
49	C 1	ARTKQTARme2aKme3STGGKAPRKQ			H3 1-19	R8me2s	K9me3			free
50	C 2	ARTKQTARme2aKacSTGGKAPRKQ			H3 1-19	R8me2s	K9ac			free
51	C 3	ARTKQTARme2aKpSTGGKAPRKQ			H3 1-19	R8me2s	S10P			free
52	C 4	ARTKQTARme2aKSpTGGKAPRKQ			H3 1-19	R8me2s	T11P			free
53	C 5	ARTKQTARme2aKme1STGGKAPRKQ			H3 1-19	R8me2a	K9me			free
54	C 6	ARTKQTARme2aKme2STGGKAPRKQ			H3 1-19	R8me2a	K9m2			free
55	C 7	ARTKQTARme2aKme3STGGKAPRKQ			H3 1-19	R8me2a	K9me3			free
56	C 8	ARTKQTARme2aKacSTGGKAPRKQ			H3 1-19	R8me2a	K9ac			free
57	C 9	ARTKQTARme2aKpSTGGKAPRKQ			H3 1-19	R8me2a	S10P			free
58	C10	ARTKQTARme2aKSpTGGKAPRKQ			H3 1-19	R8me2a	T11P			free
59	C11	ARTKQTACitKme1STGGKAPRKQ			H3 1-19	R8Citr	K9me			free
60	C12	ARTKQTACitKme2STGGKAPRKQ			H3 1-19	R8Citr	K9m2			free
61	C13	ARTKQTACitKme3STGGKAPRKQ			H3 1-19	R8Citr	K9me3			free
62	C14	ARTKQTACitKacSTGGKAPRKQ			H3 1-19	R8Citr	K9ac			free
63	C15	ARTKQTACitKpSTGGKAPRKQ			H3 1-19	R8Citr	S10P			free
64	C16	ARTKQTACitKSpTGGKAPRKQ			H3 1-19	R8Citr	T11P			free
65	C17	ARTKQTARKme1pSTGGKAPRKQ			H3 1-19	K9me	S10P			free
66	C18	ARTKQTARKme1SpTGGKAPRKQ			H3 1-19	K9me	T11P			free
67	C19	ARTKQTARKme1STGGKacAPRKQ			H3 1-19	K9me	K14ac			free
68	C20	ARTKQTARKme2pSTGGKAPRKQ			H3 1-19	K9me2	S10P			free
69	C21	ARTKQTARKme2SpTGGKAPRKQ			H3 1-19	K9me2	T11P			free
70	C22	ARTKQTARKme2STGGKacAPRKQ			H3 1-19	K9me2	K14ac			free
71	C23	ARTKQTARKme3pSTGGKAPRKQ			H3 1-19	K9me3	S10P			free
72	C24	ARTKQTARKme3SpTGGKAPRKQ			H3 1-19	K9me3	T11P			free
73	D 1	ARTKQTARKme3STGGKacAPRKQ			H3 1-19	K9me3	K14ac			free
74	D 2	ARTKQTARKacpSTGGKAPRKQ			H3 1-19	K9ac	S10P			free
75	D 3	ARTKQTARKacSpTGGKAPRKQ			H3 1-19	K9ac	T11P			free
76	D 4	ARTKQTARKacSTGGKacAPRKQ			H3 1-19	K9ac	K14ac			free
77	D 5	ARTKQTARKpSpTGGKAPRKQ			H3 1-19	S10P	T11P			free
78	D 6	ARTKQTARKpSTGGKacAPRKQ			H3 1-19	S10P	K14ac			free
79	D 7	ARTKQTARKSpTGGKacAPRKQ			H3 1-19	T11P	K14ac			free
80	D 8	ARTKQTARme2sKme1pSTGGKAPRKQ			H3 1-19	R8me2s	K9me	S10P		free
81	D 9	ARTKQTARme2sKme2pSTGGKAPRKQ			H3 1-19	R8me2s	K9me2	S10P		free
82	D10	ARTKQTARme2sKme3pSTGGKAPRKQ			H3 1-19	R8me2s	K9me3	S10P		free
83	D11	ARTKQTARme2sKacpSTGGKAPRKQ			H3 1-19	R8me2s	K9ac	S10P		free
84	D12	ARTKQTARme2sKme1SpTGGKAPRKQ			H3 1-19	R8me2s	K9me	T11P		free
85	D13	ARTKQTARme2sKme2SpTGGKAPRKQ			H3 1-19	R8me2s	K9me2	T11P		free

86	bioRxiv preprint doi: https://doi.org/10.1101/106245 ; this version posted February 6, 2017. The copyright holder for this preprint (which was not certified by peer review) is the author/funder, who has granted bioRxiv a license to display the preprint in perpetuity. It is made available under aCC-BY-NC-ND 4.0 International license.									
87	D16	A R T K Q T A Rme2a Kme1 p S T G G K A P R K Q	H3 1-19	R8me2a	K9me	S10P				free
88	D17	A R T K Q T A Rme2a Kme2 p S T G G K A P R K Q	H3 1-19	R8me2a	K9me2	S10P				free
89	D18	A R T K Q T A Rme2a Kme3 p S T G G K A P R K Q	H3 1-19	R8me2a	K9me3	S10P				free
90	D19	A R T K Q T A Rme2a Kac p S T G G K A P R K Q	H3 1-19	R8me2a	K9ac	S10P				free
91	D20	A R T K Q T A Rme2a Kme1 S p T G G K A P R K Q	H3 1-19	R8me2a	K9me	T11P				free
92	D21	A R T K Q T A Rme2a Kme2 S p T G G K A P R K Q	H3 1-19	R8me2a	K9me2	T11P				free
93	D22	A R T K Q T A Rme2a Kme3 S p T G G K A P R K Q	H3 1-19	R8me2a	K9me3	T11P				free
94	D23	A R T K Q T A Rme2a Kac S p T G G K A P R K Q	H3 1-19	R8me2a	K9ac	T11P				free
95	D24	A R T K Q T A Rme2a Kme1 p S p T G G K A P R K Q	H3 1-19	R8me2a	K9me	S10P	T11P			free
96	E 1	A R T K Q T A Rme2a Kme2 p S p T G G K A P R K Q	H3 1-19	R8me2a	K9me2	S10P	T11P			free
97	E 2	A R T K Q T A Rme2a Kme3 p S p T G G K A P R K Q	H3 1-19	R8me2a	K9me3	S10P	T11P			free
98	E 3	A R T K Q T A Rme2a Kac p S p T G G K A P R K Q	H3 1-19	R8me2a	K9ac	S10P	T11P			free
99	E 4	A Rme2s T Kme1 Q T A Rme2s K S T G G K A P R K Q	H3 1-19	R2me2s	K4me1	R8me2s				free
100	E 5	A Rme2s T Kme2 Q T A Rme2s K S T G G K A P R K Q	H3 1-19	R2me2s	K4me2	R8me2s				free
101	E 6	A Rme2s T Kme3 Q T A Rme2s K S T G G K A P R K Q	H3 1-19	R2me2s	K4me3	R8me2s				free
102	E 7	A Rme2s T Kac Q T A Rme2s K S T G G K A P R K Q	H3 1-19	R2me2s	K4ac	R8me2s				free
103	E 8	A Rme2a T Kme1 Q T A Rme2a K S T G G K A P R K Q	H3 1-19	R2me2a	K4me1	R8me2a				free
104	E 9	A Rme2a T Kme2 Q T A Rme2a K S T G G K A P R K Q	H3 1-19	R2me2a	K4me2	R8me2a				free
105	E 10	A Rme2a T Kme3 Q T A Rme2a K S T G G K A P R K Q	H3 1-19	R2me2a	K4me3	R8me2a				free
106	E 11	A Rme2a T Kac Q T A Rme2a K S T G G K A P R K Q	H3 1-19	R2me2a	K4ac	R8me2a				free
107	E 12	A Rme2s T Kme1 Q T A R Kme1 S T G G K A P R K Q	H3 1-19	R2me2s	K4me1	K9me				free
108	E 13	A Rme2s T Kme2 Q T A R Kme1 S T G G K A P R K Q	H3 1-19	R2me2s	K4me2	K9me				free
109	E 14	A Rme2s T Kme3 Q T A R Kme1 S T G G K A P R K Q	H3 1-19	R2me2s	K4me3	K9me				free
110	E 15	A Rme2s T Kac Q T A R Kme1 S T G G K A P R K Q	H3 1-19	R2me2s	K4ac	K9me				free
111	E 16	A Rme2a T Kme1 Q T A R Kme2 S T G G K A P R K Q	H3 1-19	R2me2a	K4me1	K9me2				free
112	E 17	A Rme2a T Kme2 Q T A R Kme2 S T G G K A P R K Q	H3 1-19	R2me2a	K4me2	K9me2				free
113	E 18	A Rme2a T Kme3 Q T A R Kme2 S T G G K A P R K Q	H3 1-19	R2me2a	K4me3	K9me2				free
114	E 19	A Rme2a T Kac Q T A R Kme2 S T G G K A P R K Q	H3 1-19	R2me2a	K4ac	K9me2				free
115	E 20	A Rme2s T Kme1 Q T A R Kme3 S T G G K A P R K Q	H3 1-19	R2me2s	K4me1	K9me3				free
116	E 21	A Rme2s T Kme2 Q T A R Kme3 S T G G K A P R K Q	H3 1-19	R2me2s	K4me2	K9me3				free
117	E 22	A Rme2s T Kme3 Q T A R Kme3 S T G G K A P R K Q	H3 1-19	R2me2s	K4me3	K9me3				free
118	E 23	A Rme2s T Kac Q T A R Kme3 S T G G K A P R K Q	H3 1-19	R2me2s	K4ac	K9me3				free
119	E 24	A Rme2a T Kme1 Q T A R Kac S T G G K A P R K Q	H3 1-19	R2me2a	K4me1	K9ac				free
120	F 1	A Rme2a T Kme2 Q T A R Kac S T G G K A P R K Q	H3 1-19	R2me2a	K4me2	K9ac				free
121	F 2	A Rme2a T Kme3 Q T A R Kac S T G G K A P R K Q	H3 1-19	R2me2a	K4me3	K9ac				free
122	F 3	A Rme2a T Kac Q T A R Kac S T G G K A P R K Q	H3 1-19	R2me2a	K4ac	K9ac				free
123	F 4	A R T Kme1 Q T A Rme2s Kme1 S T G G K A P R K Q	H3 1-19	K4me1	R8me2s	K9me				free
124	F 5	A R T Kme2 Q T A Rme2s Kme1 S T G G K A P R K Q	H3 1-19	K4me2	R8me2s	K9me				free
125	F 6	A R T Kme3 Q T A Rme2s Kme1 S T G G K A P R K Q	H3 1-19	K4me3	R8me2s	K9me				free
126	F 7	A R T Kac Q T A Rme2s Kme1 S T G G K A P R K Q	H3 1-19	K4ac	R8me2s	K9me				free
127	F 8	A R T Kme1 Q T A Rme2a Kme1 S T G G K A P R K Q	H3 1-19	K4me1	R8me2a	K9me				free
128	F 9	A R T Kme2 Q T A Rme2a Kme1 S T G G K A P R K Q	H3 1-19	K4me2	R8me2a	K9me				free
129	F 10	A R T Kme3 Q T A Rme2a Kme1 S T G G K A P R K Q	H3 1-19	K4me3	R8me2a	K9me				free
130	F 11	A R T Kac Q T A Rme2a Kme1 S T G G K A P R K Q	H3 1-19	K4ac	R8me2a	K9me				free
131	F 12	A R T Kme1 Q T A Rme2s Kme2 S T G G K A P R K Q	H3 1-19	K4me1	R8me2s	K9me2				free
132	F 13	A R T Kme2 Q T A Rme2s Kme2 S T G G K A P R K Q	H3 1-19	K4me2	R8me2s	K9me2				free
133	F 14	A R T Kme3 Q T A Rme2s Kme2 S T G G K A P R K Q	H3 1-19	K4me3	R8me2s	K9me2				free
134	F 15	A R T Kac Q T A Rme2s Kme2 S T G G K A P R K Q	H3 1-19	K4ac	R8me2s	K9me2				free
135	F 16	A R T Kme1 Q T A Rme2a Kme2 S T G G K A P R K Q	H3 1-19	K4me1	R8me2a	K9me2				free
136	F 17	A R T Kme2 Q T A Rme2a Kme2 S T G G K A P R K Q	H3 1-19	K4me2	R8me2a	K9me2				free
137	F 18	A R T Kme3 Q T A Rme2a Kme2 S T G G K A P R K Q	H3 1-19	K4me3	R8me2a	K9me2				free
138	F 19	A R T Kac Q T A Rme2a Kme2 S T G G K A P R K Q	H3 1-19	K4ac	R8me2a	K9me2				free
139	F 20	A R T Kme1 Q T A Rme2s Kme3 S T G G K A P R K Q	H3 1-19	K4me1	R8me2s	K9me3				free
140	F 21	A R T Kme2 Q T A Rme2s Kme3 S T G G K A P R K Q	H3 1-19	K4me2	R8me2s	K9me3				free
141	F 22	A R T Kme3 Q T A Rme2s Kme3 S T G G K A P R K Q	H3 1-19	K4me3	R8me2s	K9me3				free
142	F 23	A R T Kac Q T A Rme2s Kme3 S T G G K A P R K Q	H3 1-19	K4ac	R8me2s	K9me3				free
143	F 24	A R T Kme1 Q T A Rme2a Kme3 S T G G K A P R K Q	H3 1-19	K4me1	R8me2a	K9me3				free
144	G 1	A R T Kme2 Q T A Rme2a Kme3 S T G G K A P R K Q	H3 1-19	K4me2	R8me2a	K9me3				free
145	G 2	A R T Kme3 Q T A Rme2a Kme3 S T G G K A P R K Q	H3 1-19	K4me3	R8me2a	K9me3				free
146	G 3	A R T Kac Q T A Rme2a Kme3 S T G G K A P R K Q	H3 1-19	K4ac	R8me2a	K9me3				free
147	G 4	A R T Kme1 Q T A Rme2s Kac S T G G K A P R K Q	H3 1-19	K4me1	R8me2s	K9ac				free
148	G 5	A R T Kme2 Q T A Rme2s Kac S T G G K A P R K Q	H3 1-19	K4me2	R8me2s	K9ac				free
149	G 6	A R T Kme3 Q T A Rme2s Kac S T G G K A P R K Q	H3 1-19	K4me3	R8me2s	K9ac				free
150	G 7	A R T Kac Q T A Rme2s Kac S T G G K A P R K Q	H3 1-19	K4ac	R8me2s	K9ac				free
151	G 8	A R T Kme1 Q T A Rme2a Kac S T G G K A P R K Q	H3 1-19	K4me1	R8me2a	K9ac				free
152	G 9	A R T Kme2 Q T A Rme2a Kac S T G G K A P R K Q	H3 1-19	K4me2	R8me2a	K9ac				free
153	G 10	A R T Kme3 Q T A Rme2a Kac S T G G K A P R K Q	H3 1-19	K4me3	R8me2a	K9ac				free
154	G 11	A R T Kac Q T A Rme2a Kac S T G G K A P R K Q	H3 1-19	K4ac	R8me2a	K9ac				free
155	G 12	A Rme2s T Kme1 Q T A Rme2s Kme1 S T G G K A P R K Q	H3 1-19	R2me2s	K4me1	R8me2s	K9me			free
156	G 13	A Rme2s T Kme2 Q T A Rme2s Kme1 S T G G K A P R K Q	H3 1-19	R2me2s	K4me2	R8me2s	K9me			free
157	G 14	A Rme2s T Kme3 Q T A Rme2s Kme1 S T G G K A P R K Q	H3 1-19	R2me2s	K4me3	R8me2s	K9me			free
158	G 15	A Rme2s T Kac Q T A Rme2s Kme1 S T G G K A P R K Q	H3 1-19	R2me2s	K4ac	R8me2s	K9me			free
159	G 16	A Rme2a T Kme1 Q T A Rme2s Kme1 S T G G K A P R K Q	H3 1-19	R2me2a	K4me1	R8me2s	K9me			free
160	G 17	A Rme2a T Kme2 Q T A Rme2s Kme1 S T G G K A P R K Q	H3 1-19	R2me2a	K4me2	R8me2s	K9me			free
161	G 18	A Rme2a T Kme3 Q T A Rme2s Kme1 S T G G K A P R K Q	H3 1-19	R2me2a	K4me3	R8me2s	K9me			free
162	G 19	A Rme2a T Kac Q T A Rme2s Kme1 S T G G K A P R K Q	H3 1-19	R2me2a	K4ac	R8me2s	K9me			free
163	G 20	A Rme2s T Kme1 Q T A Rme2s Kme2 S T G G K A P R K Q	H3 1-19	R2me2s	K4me1	R8me2s	K9me2			free
164	G 21	A Rme2s T Kme2 Q T A Rme2s Kme2 S T G G K A P R K Q	H3 1-19	R2me2s	K4me2	R8me2s	K9me2			free
165	G 22	A Rme2s T Kme3 Q T A Rme2s Kme2 S T G G K A P R K Q	H3 1-19	R2me2s	K4me3	R8me2s	K9me2			free
166	G 23	A Rme2s T Kac Q T A Rme2s Kme2 S T G G K A P R K Q	H3 1-19	R2me2s	K4ac	R8me2s	K9me2			free
167	G 24	A Rme2a T Kme1 Q T A Rme2s Kme2 S T G G K A P R K Q	H3 1-19	R2me2a	K4me1	R8me2s	K9me2			free
168	H 1	A Rme2a T Kme2 Q T A Rme2s Kme2 S T G G K A P R K Q	H3 1-19	R2me2a	K4me2	R8me2s	K9me2			free
169	H 2	A Rme2a T Kme3 Q T A Rme2s Kme2 S T G G K A P R K Q	H3 1-19	R2me2a	K4me3	R8me2s	K9me2			free
170	H 3	A Rme2a T Kac Q T A Rme2s Kme2 S T G G K A P R K Q	H3 1-19	R2me2a	K4ac	R8me2s	K9me2			free
171	H 4	A Rme2s T Kme1 Q T A Rme2s Kme3 S T G G K A P R K Q	H3 1-19	R2me2s	K4me1	R8me2s	K9me3			free
172	H 5	A Rme2s T Kme2 Q T A Rme2s Kme3 S T G G K A P R K Q	H3 1-19	R2me2s	K4me2	R8me2s	K9me3			free
173	H 6	A Rme2s T Kme3 Q T A Rme2s Kme3 S T G G K A P R K Q	H3 1-19	R2me2s	K4me3	R8me2s	K9me3			free
174	H 7	A Rme2s T Kac Q T A Rme2s Kme3 S T G G K A P R K Q	H3 1-19	R2me2s	K4ac	R8me2s	K9me3			free
175	H 8	A Rme2a T Kme1 Q T A Rme2s Kme3 S T G G K A P R K Q	H3 1-19	R2me2a	K4me1	R8me2s	K9me3			free
176	H 9	A Rme2a T Kme2 Q T A Rme2s Kme3 S T G G K A P R K Q	H3 1-19	R2me2a	K4me2	R8me2s	K9me3			free
177	H 10	A Rme2a T Kme3 Q T A Rme2s Kme3 S T G G K A P R K Q	H3 1-19	R2me2a	K4me3	R8me2s	K9me3			free
178	H 11	A Rme2a T Kac Q T A Rme2s Kme3 S T G G K A P R K Q	H3 1-19	R2me2a	K4ac	R8me2s	K9me3			free

180	bioRxiv preprint doi: https://doi.org/10.1101/106245 ; this version posted February 6, 2017. The copyright holder for this preprint (which was not certified by peer review) is the author/funder, who has granted bioRxiv a license to display the preprint in perpetuity. It is made available under aCC-BY-NC-ND 4.0 International license.									
181	H14	A Rme2s T Kme3 Q T A Rme2s Kac	STGGKAPRKQ	H3 1-19	R2me2s	K4me3	R8me2s	K9ac	free	
182	H15	A Rme2s T Kac Q T A Rme2s Kac	STGGKAPRKQ	H3 1-19	R2me2s	K4ac	R8me2s	K9ac	free	
183	H16	A Rme2a T Kme1 Q T A Rme2s Kac	STGGKAPRKQ	H3 1-19	R2me2a	K4me1	R8me2s	K9ac	free	
184	H17	A Rme2a T Kme2 Q T A Rme2s Kac	STGGKAPRKQ	H3 1-19	R2me2a	K4me2	R8me2s	K9ac	free	
185	H18	A Rme2a T Kme3 Q T A Rme2s Kac	STGGKAPRKQ	H3 1-19	R2me2a	K4me3	R8me2s	K9ac	free	
186	H19	A Rme2a T Kac Q T A Rme2s Kac	STGGKAPRKQ	H3 1-19	R2me2a	K4ac	R8me2s	K9ac	free	
187	H20	A Rme2s T Kme1 Q T A Rme2a Kme1	STGGKAPRKQ	H3 1-19	R2me2s	K4me1	R8me2a	K9me	free	
188	H21	A Rme2s T Kme2 Q T A Rme2a Kme1	STGGKAPRKQ	H3 1-19	R2me2s	K4me2	R8me2a	K9me	free	
189	H22	A Rme2s T Kme3 Q T A Rme2a Kme1	STGGKAPRKQ	H3 1-19	R2me2s	K4me3	R8me2a	K9me	free	
190	H23	A Rme2s T Kac Q T A Rme2a Kme1	STGGKAPRKQ	H3 1-19	R2me2s	K4ac	R8me2a	K9me	free	
191	H24	A Rme2a T Kme1 Q T A Rme2a Kme1	STGGKAPRKQ	H3 1-19	R2me2a	K4me1	R8me2a	K9me	free	
192	I 1	A Rme2a T Kme2 Q T A Rme2a Kme1	STGGKAPRKQ	H3 1-19	R2me2a	K4me2	R8me2a	K9me	free	
193	I 2	A Rme2a T Kme3 Q T A Rme2a Kme1	STGGKAPRKQ	H3 1-19	R2me2a	K4me3	R8me2a	K9me	free	
194	I 3	A Rme2a T Kac Q T A Rme2a Kme1	STGGKAPRKQ	H3 1-19	R2me2a	K4ac	R8me2a	K9me	free	
195	I 4	A Rme2s T Kme1 Q T A Rme2a Kme2	STGGKAPRKQ	H3 1-19	R2me2s	K4me1	R8me2a	K9me2	free	
196	I 5	A Rme2s T Kme2 Q T A Rme2a Kme2	STGGKAPRKQ	H3 1-19	R2me2s	K4me2	R8me2a	K9me2	free	
197	I 6	A Rme2s T Kme3 Q T A Rme2a Kme2	STGGKAPRKQ	H3 1-19	R2me2s	K4me3	R8me2a	K9me2	free	
198	I 7	A Rme2s T Kac Q T A Rme2a Kme2	STGGKAPRKQ	H3 1-19	R2me2s	K4ac	R8me2a	K9me2	free	
199	I 8	A Rme2a T Kme1 Q T A Rme2a Kme2	STGGKAPRKQ	H3 1-19	R2me2a	K4me1	R8me2a	K9me2	free	
200	I 9	A Rme2a T Kme2 Q T A Rme2a Kme2	STGGKAPRKQ	H3 1-19	R2me2a	K4me2	R8me2a	K9me2	free	
201	I10	A Rme2a T Kme3 Q T A Rme2a Kme2	STGGKAPRKQ	H3 1-19	R2me2a	K4me3	R8me2a	K9me2	free	
202	I11	A Rme2a T Kac Q T A Rme2a Kme2	STGGKAPRKQ	H3 1-19	R2me2a	K4ac	R8me2a	K9me2	free	
203	I12	A Rme2s T Kme1 Q T A Rme2a Kme3	STGGKAPRKQ	H3 1-19	R2me2s	K4me1	R8me2a	K9me3	free	
204	I13	A Rme2s T Kme2 Q T A Rme2a Kme3	STGGKAPRKQ	H3 1-19	R2me2s	K4me2	R8me2a	K9me3	free	
205	I14	A Rme2s T Kme3 Q T A Rme2a Kme3	STGGKAPRKQ	H3 1-19	R2me2s	K4me3	R8me2a	K9me3	free	
206	I15	A Rme2s T Kac Q T A Rme2a Kme3	STGGKAPRKQ	H3 1-19	R2me2s	K4ac	R8me2a	K9me3	free	
207	I16	A Rme2a T Kme1 Q T A Rme2a Kme3	STGGKAPRKQ	H3 1-19	R2me2a	K4me1	R8me2a	K9me3	free	
208	I17	A Rme2a T Kme2 Q T A Rme2a Kme3	STGGKAPRKQ	H3 1-19	R2me2a	K4me2	R8me2a	K9me3	free	
209	I18	A Rme2a T Kme3 Q T A Rme2a Kme3	STGGKAPRKQ	H3 1-19	R2me2a	K4me3	R8me2a	K9me3	free	
210	I19	A Rme2a T Kac Q T A Rme2a Kme3	STGGKAPRKQ	H3 1-19	R2me2a	K4ac	R8me2a	K9me3	free	
211	I20	A Rme2s T Kme1 Q T A Rme2a Kac	STGGKAPRKQ	H3 1-19	R2me2s	K4me1	R8me2a	K9ac	free	
212	I21	A Rme2s T Kme2 Q T A Rme2a Kac	STGGKAPRKQ	H3 1-19	R2me2s	K4me2	R8me2a	K9ac	free	
213	I22	A Rme2s T Kme3 Q T A Rme2a Kac	STGGKAPRKQ	H3 1-19	R2me2s	K4me3	R8me2a	K9ac	free	
214	I23	A Rme2s T Kac Q T A Rme2a Kac	STGGKAPRKQ	H3 1-19	R2me2s	K4ac	R8me2a	K9ac	free	
215	I24	A Rme2a T Kme1 Q T A Rme2a Kac	STGGKAPRKQ	H3 1-19	R2me2a	K4me1	R8me2a	K9ac	free	
216	J 1	A Rme2a T Kme2 Q T A Rme2a Kac	STGGKAPRKQ	H3 1-19	R2me2a	K4me2	R8me2a	K9ac	free	
217	J 2	A Rme2a T Kme3 Q T A Rme2a Kac	STGGKAPRKQ	H3 1-19	R2me2a	K4me3	R8me2a	K9ac	free	
218	J 3	A Rme2a T Kac Q T A Rme2a Kac	STGGKAPRKQ	H3 1-19	R2me2a	K4ac	R8me2a	K9ac	free	
219	J 4	ARKSTGGKAPRKQLATKAAR		H3 7-26	unmod				acetylated	
220	J 5	ARKSTGGKacAPRKQLATKAAR		H3 7-26	K14ac				acetylated	
221	J 6	ARKpSTGGKacAPRKQLATKAAR		H3 7-26	K14ac	S10P			acetylated	
222	J 7	ARKSpTGGKacAPRKQLATKAAR		H3 7-26	K14ac	T11P			acetylated	
223	J 8	ARKSTGGKAPRme2sKQLATKAAR		H3 7-26	R17me2s				acetylated	
224	J 9	ARKSTGGKAPRme2aKQLATKAAR		H3 7-26	R17me2a				acetylated	
225	J10	ARKSTGGKAPCitKQLATKAAR		H3 7-26	R17Citr				acetylated	
226	J11	ARKSTGGKAPRKacQLATKAAR		H3 7-26	K18Ac				acetylated	
227	J12	ARKSTGGKacAPRme2sKQLATKAAR		H3 7-26	K14ac	R17me2s			acetylated	
228	J13	ARKSTGGKacAPRme2aKQLATKAAR		H3 7-26	K14ac	R17me2a			acetylated	
229	J14	ARKSTGGKacAPRKacQLATKAAR		H3 7-26	K14ac	K18Ac			acetylated	
230	J15	ARKSTGGKAPRme2sKacQLATKAAR		H3 7-26	R17me2s	K18Ac			acetylated	
231	J16	ARKSTGGKAPRme2aKacQLATKAAR		H3 7-26	R17me2a	K18Ac			acetylated	
232	J17	ARKSTGGKAPCitKacQLATKAAR		H3 7-26	R17Citr	K18Ac			acetylated	
233	J18	ARKSTGGKacAPRme2sKacQLATKAAR		H3 7-26	K14ac	R17me2s	K18Ac		acetylated	
234	J19	ARKSTGGKacAPRme2aKacQLATKAAR		H3 7-26	K14ac	R17me2a	K18Ac		acetylated	
235	J20	PRKQLATKAARKSAPATGG		H3 16-35	unmod				acetylated	
236	J21	PRKQLATKAARme2sKSAPATGG		H3 16-35	R26me2s				acetylated	
237	J22	PRKQLATKAARme2aKSAPATGG		H3 16-35	R26me2a				acetylated	
238	J23	PRKQLATKAACitKSAPATGG		H3 16-35	R26Citr				acetylated	
239	J24	PRKQLATKAARKme1SAPATGG		H3 16-35	K27me				acetylated	
240	K 1	PRKQLATKAARKme2SAPATGG		H3 16-35	K27me2				acetylated	
241	K 2	PRKQLATKAARKme3SAPATGG		H3 16-35	K27me3				acetylated	
242	K 3	PRKQLATKAARKacSAPATGG		H3 16-35	K27ac				acetylated	
243	K 4	PRKQLATKAARKpSAPATGG		H3 16-35	S28P				acetylated	
244	K 5	PRKQLATKAARme2sKme1SAPATGG		H3 16-35	R26me2s	K27me			acetylated	
245	K 6	PRKQLATKAARme2sKme2SAPATGG		H3 16-35	R26me2s	K27me2			acetylated	
246	K 7	PRKQLATKAARme2sKme3SAPATGG		H3 16-35	R26me2s	K27me3			acetylated	
247	K 8	PRKQLATKAARme2sKacSAPATGG		H3 16-35	R26me2s	K27ac			acetylated	
248	K 9	PRKQLATKAARme2sKpSAPATGG		H3 16-35	R26me2s	S28P			acetylated	
249	K10	PRKQLATKAARme2aKme1SAPATGG		H3 16-35	R26me2a	K27me			acetylated	
250	K11	PRKQLATKAARme2aKme2SAPATGG		H3 16-35	R26me2a	K27me2			acetylated	
251	K12	PRKQLATKAARme2aKme3SAPATGG		H3 16-35	R26me2a	K27me3			acetylated	
252	K13	PRKQLATKAARme2aKacSAPATGG		H3 16-35	R26me2a	K27ac			acetylated	
253	K14	PRKQLATKAARme2aKpSAPATGG		H3 16-35	R26me2a	S28P			acetylated	
254	K15	PRKQLATKAACitKme1SAPATGG		H3 16-35	R26Citr	K27me			acetylated	
255	K16	PRKQLATKAACitKme2SAPATGG		H3 16-35	R26Citr	K27me2			acetylated	
256	K17	PRKQLATKAACitKme3SAPATGG		H3 16-35	R26Citr	K27me3			acetylated	
257	K18	PRKQLATKAACitKpSAPATGG		H3 16-35	R26Citr	S28P			acetylated	
258	K19	PRKQLATKAARKme1pSAPATGG		H3 16-35	K27me	S28P			acetylated	
259	K20	PRKQLATKAARKme2pSAPATGG		H3 16-35	K27me2	S28P			acetylated	
260	K21	PRKQLATKAARKme3pSAPATGG		H3 16-35	K27me3	S28P			acetylated	
261	K22	PRKQLATKAARKacpSAPATGG		H3 16-35	K27ac	S28P			acetylated	
262	K23	PRKQLATKAARme2sKme1pSAPATGG		H3 16-35	R26me2s	K27me	S28P		acetylated	
263	K24	PRKQLATKAARme2sKme2pSAPATGG		H3 16-35	R26me2s	K27me2	S28P		acetylated	
264	L 1	PRKQLATKAARme2sKme3pSAPATGG		H3 16-35	R26me2s	K27me3	S28P		acetylated	
265	L 2	PRKQLATKAARme2sKacpSAPATGG		H3 16-35	R26me2s	K27ac	S28P		acetylated	
266	L 3	PRKQLATKAARme2aKme1pSAPATGG		H3 16-35	R26me2a	K27me	S28P		acetylated	
267	L 4	PRKQLATKAARme2aKme2pSAPATGG		H3 16-35	R26me2a	K27me2	S28P		acetylated	
268	L 5	PRKQLATKAARme2aKme3pSAPATGG		H3 16-35	R26me2a	K27me3	S28P		acetylated	
269	L 6	PRKQLATKAARme2aKacpSAPATGG		H3 16-35	R26me2a	K27ac	S28P		acetylated	
270	L 7	RKSAPATGGVKKPHRYRPG		H3 26-45	unmod				acetylated	
271	L 8	RKSAPATGGVKme1KPHRYRPG		H3 26-45	K36me				acetylated	
272	L 9	RKSAPATGGVKme2KPHRYRPG		H3 26-45	K36me2				acetylated	

274	<p>bioRxiv preprint doi: https://doi.org/10.1101/106245; this version posted February 2, 2017. The copyright holder for this preprint (which was not certified by peer review) is the author/funder, who has granted bioRxiv a license to display the preprint in perpetuity. It is made available under aCC-BY-NC-ND 4.0 International license.</p>									
275	L12	SGRGKGGKGLGKGGAKRHR								
276	L13	pSGRGKGGKGLGKGGAKRHR	H4 1-19	unmod						free
277	L14	SGRme2s G K G G K G L G K G G A K R H R	H4 1-19	S1P						free
278	L15	SGRme2a G K G G K G L G K G G A K R H R	H4 1-19	R3me2s						free
279	L16	SGRGKac G K G K L G K G G A K R H R	H4 1-19	R3me2a						free
280	L17	SGRGKGGKac GLGKGGAKRHR	H4 1-19	K5ac						free
281	L18	SGRGKGGKGLGKac GGAKRHR	H4 1-19	K8ac						free
282	L19	SGRGKGGKGLGKac GGAKRHR	H4 1-19	K12ac						free
283	L20	SGRGKGGKGLGKac GGAKRHR	H4 1-19	K16ac						free
284	L21	pSGRme2s G K G G K G L G K G G A K R H R	H4 1-19	S1P	R3me2s					free
285	L22	pSGRme2a G K G G K G L G K G G A K R H R	H4 1-19	S1P	R3me2a					free
286	L23	pSGRGKac G K G K L G K G G A K R H R	H4 1-19	S1P	K5ac					free
287	L24	SGRme2s G Kac G K G K L G K G G A K R H R	H4 1-19	R3me2s	K5ac					free
288	M1	SGRme2s G K G G Kac GLGKGGAKRHR	H4 1-19	R3me2s	K8ac					free
289	M2	SGRme2a G Kac G K G K L G K G G A K R H R	H4 1-19	R3me2a	K5ac					free
290	M3	SGRGKac G G Kac GLGKGGAKRHR	H4 1-19	R3me2a	K8ac					free
291	M4	SGRGKGGKac GLGKac GGAKRHR	H4 1-19	K5ac	K8ac					free
292	M5	SGRGKGGKac GLGKac GGAKRHR	H4 1-19	K8ac	K12ac					free
293	M6	SGRGKGGKGLGKac GGAKRHR	H4 1-19	K8ac	K16ac					free
294	M7	pSGRme2s G Kac G K G K L G K G G A K R H R	H4 1-19	K12ac	K16ac					free
295	M8	pSGRme2a G Kac G K G K L G K G G A K R H R	H4 1-19	S1P	R3me2s	K5ac				free
296	M9	SGRme2s G Kac G G Kac GLGKGGAKRHR	H4 1-19	S1P	R3me2a	K5ac				free
297	M10	SGRme2a G Kac G G Kac GLGKGGAKRHR	H4 1-19	R3me2s	K5ac	K8ac				free
298	M11	SGRGKac G G Kac GLGKac GGAKRHR	H4 1-19	R3me2a	K5ac	K8ac				free
299	M12	SGRGKGGKac GLGKac GGAKRHR	H4 1-19	K5ac	K8ac	K12ac				free
300	M13	SGRGKGGKac GLGKac GGAKRHR	H4 1-19	K8ac	K12ac	K16ac				free
301	M14	pSGRme2s G Kac G G Kac GLGKGGAKRHR	H4 1-19	S1P	R3me2s	K5ac	K8ac			free
302	M15	pSGRme2a G Kac G G Kac GLGKGGAKRHR	H4 1-19	S1P	R3me2a	K5ac	K8ac			free
303	M16	SGRme2s G Kac G G Kac GLGKGGAKRHR	H4 1-19	R3me2s	K5ac	K8ac	K12ac			free
304	M17	SGRme2a G Kac G G Kac GLGKGGAKRHR	H4 1-19	R3me2a	K5ac	K8ac	K12ac			free
305	M18	SGRGKac G G Kac GLGKac GGAKRHR	H4 1-19	K5ac	K8ac	K12ac	K16ac			free
306	M19	GKGGAKRHRKVL RDNIQGIT	H4 11-30	unmod						acetylated
307	M20	GKac GGA KRHRKVL RDNIQGIT	H4 11-30	K12ac						acetylated
308	M21	GKGGAK Rme2s HRKVL RDNIQGIT	H4 11-30	K16ac						acetylated
309	M22	GKGGAK Rme2a HRKVL RDNIQGIT	H4 11-30	R17me2s						acetylated
310	M23	GKGGAK Rme2a HRKVL RDNIQGIT	H4 11-30	R17me2a						acetylated
311	M24	GKGGAK Rme2s KVL RDNIQGIT	H4 11-30	R19me2s						acetylated
312	N1	GKGGAK RHR Kme1 VL RDNIQGIT	H4 11-30	R19me2a						acetylated
313	N2	GKGGAK RHR Kme2 VL RDNIQGIT	H4 11-30	K20me1						acetylated
314	N3	GKGGAK RHR Kme3 VL RDNIQGIT	H4 11-30	K20me2						acetylated
315	N4	GKGGAK RHR Kme3 VL RDNIQGIT	H4 11-30	K20me3						acetylated
316	N5	GKGGAK RHR Kac VL RDNIQGIT	H4 11-30	K20ac						acetylated
317	N6	GKGGAK RHR KVL Rme2a DNIQGIT	H4 11-30	R24me2a						acetylated
318	N7	GKGGAK RHR KVL Rme2s DNIQGIT	H4 11-30	R24me2s						acetylated
319	N8	GKac GGA Kac RHRKVL RDNIQGIT	H4 11-30	K12ac	K16ac					acetylated
320	N9	GKGGAKac Rme2s HRKVL RDNIQGIT	H4 11-30	K16ac	R17me2s					acetylated
321	N10	GKGGAKac Rme2a HRKVL RDNIQGIT	H4 11-30	K16ac	R17me2a					acetylated
322	N11	GKGGAKac RHR Rme2s KVL RDNIQGIT	H4 11-30	K16ac	R19me2s					acetylated
323	N12	GKGGAKac RHR Rme2a KVL RDNIQGIT	H4 11-30	K16ac	R19me2a					acetylated
324	N13	GKGGAKac RHR Kme1 VL RDNIQGIT	H4 11-30	K16ac	K20me1					acetylated
325	N14	GKGGAKac RHR Kme2 VL RDNIQGIT	H4 11-30	K16ac	K20me2					acetylated
326	N15	GKGGAKac RHR Kme3 VL RDNIQGIT	H4 11-30	K16ac	K20me3					acetylated
327	N16	GKGGAKac RHR Kac VL RDNIQGIT	H4 11-30	K16ac	K20ac					acetylated
328	N17	GKac GGA Kac RHR Kme1 VL RDNIQGIT	H4 11-30	K12ac	K16ac	K20me1				acetylated
329	N18	GKac GGA Kac RHR Kme2 VL RDNIQGIT	H4 11-30	K12ac	K16ac	K20me2				acetylated
330	N19	GKac GGA Kac RHR Kme3 VL RDNIQGIT	H4 11-30	K12ac	K16ac	K20me3				acetylated
331	N20	GKac GGA Kac RHR Kac VL RDNIQGIT	H4 11-30	K12ac	K16ac	K20ac				acetylated
332	N21	GKGGAK RHR Rme2a Kme1 VL RDNIQGIT	H4 11-30	R19me2a	K20me1					acetylated
333	N22	GKGGAK RHR Rme2a Kme2 VL RDNIQGIT	H4 11-30	R19me2a	K20me2					acetylated
334	N23	GKGGAK RHR Rme2a Kme3 VL RDNIQGIT	H4 11-30	R19me2a	K20me3					acetylated
335	N24	GKGGAK RHR Rme2a Kac VL RDNIQGIT	H4 11-30	R19me2a	K20ac					acetylated
336	O1	GKGGAK RHR Rme2s Kme1 VL RDNIQGIT	H4 11-30	R19me2s	K20me1					acetylated
337	O2	GKGGAK RHR Rme2s Kme2 VL RDNIQGIT	H4 11-30	R19me2s	K20me2					acetylated
338	O3	GKGGAK RHR Rme2s Kme3 VL RDNIQGIT	H4 11-30	R19me2s	K20me3					acetylated
339	O4	GKGGAK RHR Rme2s Kac VL RDNIQGIT	H4 11-30	R19me2s	K20ac					acetylated
340	O5	GKGGAK RHR Kme1 VL Rme2a DNIQGIT	H4 11-30	R24me2a	K20me1					acetylated
341	O6	GKGGAK RHR Kme2 VL Rme2a DNIQGIT	H4 11-30	R24me2a	K20me2					acetylated
342	O7	GKGGAK RHR Kme3 VL Rme2a DNIQGIT	H4 11-30	R24me2a	K20me3					acetylated
343	O8	GKGGAK RHR Kac VL Rme2a DNIQGIT	H4 11-30	R24me2a	K20ac					acetylated
344	O9	GKGGAK RHR Kme1 VL Rme2s DNIQGIT	H4 11-30	R24me2s	K20me1					acetylated
345	O10	GKGGAK RHR Kme2 VL Rme2s DNIQGIT	H4 11-30	R24me2s	K20me2					acetylated
346	O11	GKGGAK RHR Kme3 VL Rme2s DNIQGIT	H4 11-30	R24me2s	K20me3					acetylated
347	O12	GKGGAK RHR Kac VL Rme2s DNIQGIT	H4 11-30	R24me2s	K20ac					acetylated
348	O13	SGRGKQGGKARAKAKSRSS	H2a 1-19	unmod						free
349	O14	pSGRGKQGGKARAKAKSRSS	H2a 1-19	S1P						free
350	O15	SGRGKac QGGKARAKAKSRSS	H2a 1-19	K5ac						free
351	O16	SGRGKQGGKac ARAKAKSRSS	H2a 1-19	K9ac						free
352	O17	SGRGKQGGKac ARAKAKSRSS	H2a 1-19	K13ac						free
353	O18	pSGRGKac QGGKARAKAKSRSS	H2a 1-19	S1P	K5ac					free
354	O19	pSGRGKQGGKac ARAKAKSRSS	H2a 1-19	S1P	K9ac					free
355	O20	pSGRGKQGGKac ARAKAKSRSS	H2a 1-19	S1P	K13ac					free
356	O21	SGRGKac QGGKac ARAKAKSRSS	H2a 1-19	K5ac	K9ac					free
357	O22	SGRGKQGGKac ARAKAKSRSS	H2a 1-19	K5ac	K13ac					free
358	O23	SGRGKQGGKac ARAKAKSRSS	H2a 1-19	K9ac	K13ac					free
359	O24	pSGRGKac QGGKac ARAKAKSRSS	H2a 1-19	S1P	K5ac	K9ac				free
360	P1	pSGRGKQGGKac ARAKAKSRSS	H2a 1-19	S1P	K5ac	K13ac				free
361	P2	SGRGKac QGGKac ARAKAKSRSS	H2a 1-19	S1P	K9ac	K13ac				free
362	P3	SGRGKQGGKac ARAKAKSRSS	H2a 1-19	K5ac	K9ac	K13ac				free
363	P4	pSGRGKac QGGKac ARAKAKSRSS	H2a 1-19	S1P	K5ac	K9ac	K13ac			free
364	P5	PDPAKSAPAPKKGSKKAVT	H2B 1-19	unmod						free
365	P6	PDPAKac SAPAPKKGSKKAVT	H2B 1-19	K5ac						free
366	P7	PDPAKSAPAPKKGSKKAVT	H2B 1-19	K12ac						free
367			H2B 1-19	S14P						free

